energy&fuels

pubs.acs.org/EF

Article

Interfacial Material in Water-in-Oil Emulsions Characterized by ESI(−) FT-ICR MS: Evaluation of the Influence of Centrifugation Conditions

Luciara C. Souza, Lindamara M. Souza, Eliane V. Barros, Emily A. Carvalho, Marcos H. O. Petroni, Gabriely S. Folli, Cristina M. S. Sad, Danielle M. M. Franco, Gabriel H. M. Dufrayer, Boniek G. Vaz, Marcio N. Souza, Osvaldo Karnitz, Jr., Luiz S. Chinelatto, Jr., Marcia C. K. Oliveira, Valdemar Lacerda, Jr., and Wanderson Romão*

Cite This: *Energy Fuels* 2025, 39, 18773−18790

Read Online

ACCESS | Metrics & More | Article Recommendations | Supporting Information

ABSTRACT: Emulsion represents a major challenge in the petroleum industry due to its stabilization promoted by polar fractions. In this study, interfacial material (IM) residues were isolated from a naturally emulsified crude oil using a centrifugation-based methodology under different times and temperature conditions. The recovered interfacial materials were characterized by negative-ion electrospray Fourier transform ion cyclotron resonance mass spectrometry (ESI(−) FT-ICR MS). Results showed that longer centrifugation times and higher temperatures reduced the abundance of nitrogen species while enriching oxygenated classes, particularly naphthenic acids and mixed heteroatomic species. Highly aromatic compounds migrated into $NO_2[H]$ and $NO_3[H]$ classes, whereas both linear and aromatic naphthenic acids, $O_2[H]$ class, became more prominent. Van Krevelen diagrams confirmed the increase in aromaticity of the IMR compared with the original emulsion. These findings highlight the role of centrifugation parameters in modulating the composition of IM and provide new insights into the molecular species responsible for emulsion stability.

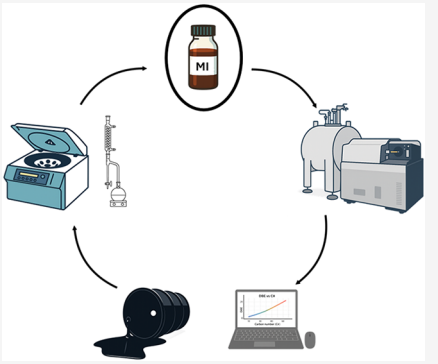

1. INTRODUCTION

In the oil industry, there are several challenges related to the extraction, production, transportation, processing, and refining of oil. These include the formation of stable water-in-oil (W/O) emulsions, which directly affect crude oil flow and processing.[1−3] An emulsion is a colloidal dispersion between two immiscible liquids, where one liquid is dispersed as a droplet inside the other liquid (continuous phase).[1,4] In the case of W/O emulsions, the water droplets, usually from the formation or secondary recovery water, are dispersed in the oil phase, called the continuous phase. There are also so-called inverse emulsions, which are of the O/W type, where oil droplets are dispersed in water.[1,4] These emulsions are thermodynamically unstable dispersions whose variation in Gibbs free energy implies a spontaneous process for separating the phases.[5] However, the presence of stabilizing species, such as emulsifiers, can provide greater stability for these dispersions.[1,4,5] In oil emulsions, the main natural emulsifiers are asphaltenes, resins, naphthenic acids, and waxes, which promote an increase in emulsion stability through the formation of interfacial films, which form the interfacial material (IM).[1−3,5−9] Polar species, such as asphaltenes and resins, play a fundamental role in reducing interfacial tension (IFT), while solid species, such as fine particles or wax crystals, promote an increase in the structural strength of the interfacial film.[1,4,6,10,11] A lower interfacial tension promotes greater stability for the suspended droplets, while a greater structural resistance of the interface makes it more difficult for the interfacial film to break and consequently coalesce, as coalescence is one of the main mechanisms responsible for destabilizing emulsions. When it occurs, it leads to the formation of larger droplets, eventually resulting in the separation of the phases.[4,12] In this way, phase separation of W/O emulsions is particularly difficult when these species are present in the interfacial film, which demonstrates the importance of studying the chemical constitution of the material acting at the interface, *i.e.*, the IM.

For the indirect study of the IM in W/O emulsions, different methods are generally used to investigate the interface using rheology techniques to determine the viscosity and interfacial viscoelasticity by dynamic stress.[13,14] However, to fully

Received: July 14, 2025
Revised: September 15, 2025
Accepted: September 18, 2025
Published: September 23, 2025

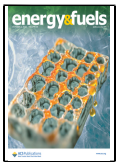

https://doi.org/10.1021/acs.energyfuels.5c03699
Energy Fuels 2025, 39, 18773−18790

elucidate the species that act at the interface, it is appropriate to specifically explore the species adsorbed on water droplets, especially in compositional terms. Therefore, methodologies for the extraction and isolation of IM are of great importance for a better understanding of the chemical identity of the species that mainly act in the stabilization of emulsions. Different methodologies for IM isolation have been reported in the literature. These include the use of heavy water (D_2O) to form a moist cake with water and IM,[15] the use of wet silica, which consists of using a column of silica with controlled humidity to adsorb the interfacially active species,[16] and the centrifugation method using the Dean−Stark technique.[17] The latter methodology, developed in 2014 by Pereira et al.,[17] consists of centrifuging the emulsions to ideally generate two phases: The oily supernatant (top) and the unresolved phase (residue that has become sedimented). The sedimented residue has a high aqueous phase content, and consequently, an abundance is enriched in interfacially active species. Therefore, after extracting this residue and removing the water, it provides the main species present at the interface of the water droplets.[18−21]

Among the studies that evaluated the interfacially active species, the work carried out by Jarvis et al. (2015)[16] used the wet silica method, applied to Arabian heavy crude, Gulf of Mexico, Athabasca bitumen, and the negative-ion mode electrospray Fourier transform ion cyclotron resonance mass spectrometry (ESI(−) FT-ICR MS) technique. The authors reported that the predominant classes at the interface are oxygenated (such as O_2) and mixed classes containing oxygen and sulfur atoms (O_xS_y, where x = 1−5 and y = 1−2).

Lalli et al. (2017)[22] applied the wet silica method to a sample of Athabasca bitumen and a heavy crude oil to investigate the presence of functional isomers in the IM of W/O emulsions. The samples were analyzed using ion mobility mass spectrometry (IM-MS) combined with collision-induced dissociation after ion mobility (CID MS). Lalli et al. (2017)[22] characterized IM with a time-of-flight (TOF) MS analyzer, evidencing multiple isomeric species of the O_3S_1 class for both samples. The authors used the high accuracy of the FT-ICR MS technique, and their results corroborate the data obtained by TOF MS. In addition, natural O_3S_1 groups were predominantly detected in the IM of the emulsion of the Athabasca bitumen sample. They can correspond to linear alkylbenzenesulfonate (LAS) surfactants, which are used in petroleum operations. The efficiency of the wet silica method for isolating and characterizing interfacially active species was systematically investigated using ESI(−) FT-ICR MS in other studies.[23,24] The method proved to be highly effective in the selective extraction of both synthetic and natural surfactant species present in petroleum sulfonate extracts. Analysis by FT-ICR MS allowed for the identification of the O_3S and $O_3S + X$ classes (where X can be sulfur, oxygen, or nitrogen), confirming their structural characteristics and surfactant nature. Investigation of the relationship between the structure of surface-active species and interfacial tension revealed a significant dependence between interfacial tension, emulsion stability, and the molecular weight of the interfacial material (IM). The analysis showed that $O_3S + X$ sulfonates interact with the aqueous phase, corroborating their surface-active activity, while organic acids did not show significant surface activity.[23,24]

Wu et al. (2022)[25] applied the wet silica method to crude oil samples from three locations in China to obtain IM and used the Orbitrap MS technique combined with CID to identify the IM functional groups. The authors found predominantly the O_4 (attributed to dicarboxylic acids and their salts), O_3S_1 (sulfonates), O_4S_1 (sulfonates or sulfates), and N_1O_2 (amphipathic molecules with carboxylic and pyridyl functional groups) classes.

The IM obtained by the wet silica method can be characterized using other analytical techniques, such as infrared spectroscopy (FTIR), liquid chromatography coupled to mass spectrometry (LC-MS), and high-resolution mass spectrometry by inductively coupled plasma gel permeation chromatography (GPC ICP HR MS).[27]

In this context, Norrman and coauthors (2020)[28] isolated the IM, using the method of Jarvis et al. (2015) with adaptations, and characterized it using FTIR and LC-MS techniques. The authors confirmed the presence of mixed polarities compounds: the most polar include naphthenic acids, the least polar are nitrogen-containing aromatic bases (such as pyridines, quinolines, pyrroles, indoles, indolines, and carbazoles), as well as compounds with polarities between those of acids and bases (such as phenols, pyrans, benzopyrans, naphthopyrans, benzonaphthopyrans, dibenzopyrans, dinaphthopyrans, and compounds containing nitrogen and oxygen atoms).

Ligiero et al. (2017)[27] used the GPC ICP HR MS technique to analyze the size distributions of IM molecules from four oils isolated using the wet silica method. Successive extractions were carried out, which concentrated larger and more insoluble compounds containing sulfur (S), vanadium (V), and nickel (Ni). For the compounds containing Ni and V at the W/O interface, the same profiles were identified for the four samples containing high M_w molecules. The sulfur compounds showed unique profiles for each oil. The authors therefore concluded that there is a correlation between S-containing aggregates and the stability of the crude oil emulsion. They also concluded that high M_w compounds could stabilize these emulsions, and/or medium and low M_w compounds could help destabilize W/O emulsions.

The method of Pereira et al. (2014)[17] combined centrifugation and distillation with Dean−Stark glassware to separate the IM (emulsion phase extracts). The composition of the IM was obtained by ESI(−) FT-ICR MS and was correlated with the stability of the emulsions. The authors identified the $N_1[H]$ class (presence of the benzo- and dibenzocarbazole series with a DBE of 12 and 15 and m/z 200−360 and other nitrogen compounds, m/z > 300) as the most abundant in the crude oil samples and the emulsion phase extracts. The IMs also showed the O[H] class (phenols) and acidic components, such as the O_2, the O_4, the O_4S, and the NO_x classes (N_1O_1 and N_1O_2). They therefore concluded that compounds with surface activity would have at least one oxygen atom. They associated the high relative abundance of the O_1 and O_2 classes with greater emulsion stability and viscosity. And they reported that the high value of the O_1/O_2 ratio results in the formation of waxy gel emulsions.

Therefore, it has been shown that a suitable extraction method combined with a compositional analysis of the IM generates a satisfactory understanding of the identity of the important interfacial species in an oil emulsion. In this sense, the use of the ESI(−) FT-ICR MS is ideal for understanding which molecules and groups are present and active in the chemical composition of the IM.[27−29]

https://doi.org/10.1021/acs.energyfuels.5c03699
Energy Fuels 2025, 39, 18773−18790

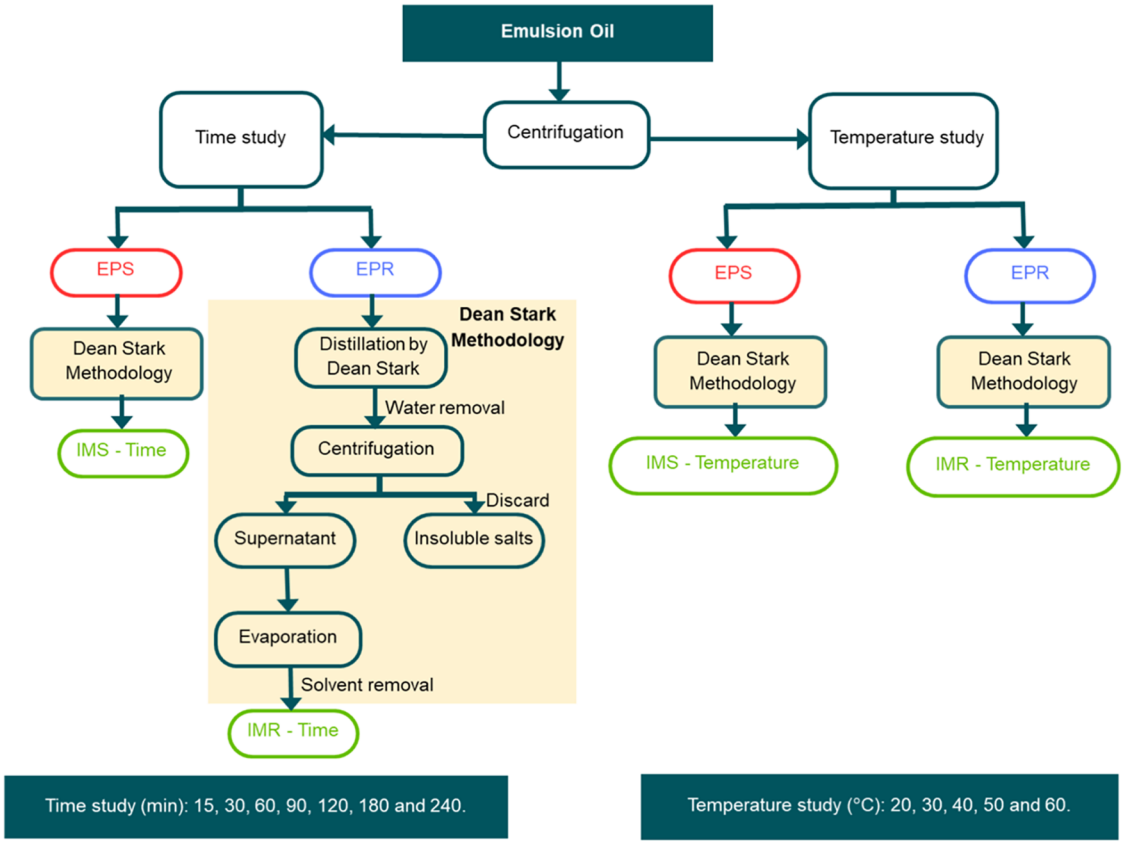

Figure 1. Diagram of the fractions obtained by optimizing the centrifugation time and temperature using the Dean−Stark method.

According to the literature, the wet silica method has been widely explored for the extraction and chemical identification of IM, while the heavy water method has high complexity, low yield, and limited reproducibility and is less widely used.[23] Thus, the centrifugation methodology is satisfactorily applicable,[17] allowing the isolation of active compounds, which are responsible for stabilizing the emulsion. The separation of the oily, aqueous, and emulsion phases facilitates the concentration of stabilizing components, such as naphthenic acids, asphaltenes, and *n*-paraffins, which are essential for the accurate analysis of these components. Dean−Stark distillation using xylene contributes to the efficient removal of water from the emulsion phase, increasing the concentration of polar compounds and preventing these species from being overlooked during analysis.

Although still rarely applied, the methodology[17] has been optimized to provide a more detailed understanding of the composition of interfacial materials, allowing significant advances in the analysis of their characteristics. The main innovation of this work consists of evaluating the influence of time (from 15 to 240 min) and temperature (from 20 to 60 °C) during centrifugation at a rotation speed of 9500 rpm. This adjustment aims to improve the efficiency of phase separation, as well as allow the concentration of interfacial compounds, favoring the migration of polar compounds, and providing a more precise analysis of IM. The centrifugation method, by promoting the concentration of species in a single phase (EPR), followed by the selective removal of water and solids, is better able to preserve the representativeness of interfacial species. This includes not only the species that are directly adsorbed at the interface of the water droplets but also those located in external adsorption layers, which play an important role in the stability of the emulsion. With this optimization, it is hoped to improve understanding of the mechanisms governing the formation and stabilization of emulsions, as well as identifying critical compounds such as naphthenic acids, asphaltenes, and other polar compounds present at the interface. ESI(−) FT-ICR MS analysis detailed the characterization of the compounds present, providing information on their composition and molecular structure.

2. EXPERIMENTAL SECTION

2.1. Sample. This study used a sample of crude oil emulsion supplied by the Leopoldo Américo Miguez de Mello Research, Development and Innovation Centre (CENPES/Petrobras - Rio de Janeiro, RJ, Brazil), previously characterized and used in the literature.[30−3132] The oil was characterized at the Petroleum Characterization and Processing Laboratory (LCP), located at the Petroleum Chemistry Competence Center (NCQP-LABPETRO), a supplementary body to the Exact Sciences Center of the Federal University of Espírito Santo (UFES).

The crude oil samples were analyzed on a Thermo Fisher Scientific Trace 1610 chromatograph. Following the methodology adapted from Coutinho et al.,[43] for crude oil analysis by GC-FID, split injection (split ratio, 1:20) of 1 μL using a HP-5MS capillary silica column (Agilent Technologies, Palo Alto, CA) and 5% phenyl−95% methylsiloxane (30 m, 0.25 mm i.d., 0.25 μm df) was thrown, with helium (99.99% purity) as the carrier gas at 1.0 mL/min. The GC oven temperature program was 40 to 320 °C at 6 °C/min and held at 310 °C for 10 min. The injector temperature was 310 °C, and the detector temperature was 350 °C.

2.2. Reagents. Reagents such as toluene were purchased from Sigma-Aldrich 99.9%, (St. Louis, MO), xylene (Neon, P.A/ACS), and methanol (MeOH, 99.9%) was acquired from Vetec Fine Chemicals, Inc. (Rio de Janeiro, Brazil), and sodium trifluoroacetate (98%,

https://doi.org/10.1021/acs.energyfuels.5c03699
Energy Fuels 2025, 39, 18773−18790

NaTFA) and ammonium hydroxide (28%, NH_4OH) were purchased from Sigma-Aldrich Chemicals (St. Louis, MO). All reagents used in the analyses were used as received without any further purification.

2.3. Extraction of Interfacial Material. The extraction of interfacial material (IM) followed a procedure adapted from Pereira et al.[17] In summary, the emulsified oil was centrifuged at 9,500 rpm to promote phase separation into a resolved supernatant phase (EPS) and an unresolved residual phase (EPR). The EPS was carefully collected by pipetting the upper layer to avoid contamination, and its clarity was visually inspected to ensure the absence of residual oil droplets. When turbidity was detected, the fraction was recentrifuged until a clear phase was obtained. Both the EPS and EPR were subsequently processed by Dean−Stark distillation, followed by a second centrifugation to remove salts. Solvent evaporation produced interfacial material from the EPS (IMS) and EPR (IMR) (Figure 1). The influence of centrifugation parameters was evaluated by varying the time (15 to 240 min at 60 °C) and temperature (20 to 60 °C for 120 min), maintaining a constant rotation speed of 9500 rpm.

2.4. ESI(−) FT-ICR MS. Samples were analyzed using a Solarix 7T FT-ICR MS instrument (Bruker Daltonics, Bremen, Germany), which was equipped with an electrospray ionization source that operated in negative-ion mode. Solutions of 0.5 mg/mL in a toluene/methanol mixture (1:1 v/v) containing 0.1% ammonium hydroxide were infused directly at a rate of 4 μL/min over an m/z range of 120−2000. External calibration using NaTFA yielded a resolving power of 8.5−8.8 × 10^5 at m/z 400 and a mass accuracy of less than 1 ppm. This enabled the reliable assignment of molecular formulas for singly charged ions. Source and acquisition parameters are detailed in the Supporting Information. The spectra were recalibrated using homologous alkylated compounds in Data Analysis 4.0 (Bruker), and the molecular formula assignments were performed with Composer software (Sierra Analytics) following established petroleomics protocols.[45,46,48−50]

The mass spectra were processed using an algorithm specifically developed for signal processing in the Composer software (Sierra Analytics, Modesto, CA).[51] The graphs were generated using the Thanus software, developed at LaCEM-UFG.[52] The elemental composition was determined from the m/z values obtained from the mass spectra. The results were represented in distribution plots to facilitate analysis, including heteroatom compound class distributions, double bond equivalent (DBE) profiles by relative abundance for selected classes, carbon number distributions by relative intensity, DBE versus carbon number plots, and Van Krevelen diagrams. These visualization tools enable a comprehensive overview of molecular features and facilitate the interpretation of MS results. The DBE values, which indicate the degree of unsaturation and hydrogen deficiency of each compound, were determined following well-established approaches in the literature.[53−56] The average molecular weight (M_w) of the detected species was calculated by the Composer software based on the relative contribution of individual ion peaks, as commonly applied in petroleomics and complex mixture analysis.[22,47]

3. RESULTS AND DISCUSSION

3.1. Physical and Chemical Properties of Oil. Table 1 summarizes the physical and chemical properties of the crude oil. Analysis of the crude oil emulsion revealed a high BS&W content of 54.4% v/v, confirming the predominance of a W/O (water-in-oil) profile. The presence of high levels of water and solids is consistent with the formation of highly stable interfacial films that are difficult to break under conventional separation conditions. Following dehydration, the residual water content fell below 0.5% v/v, meeting standard specifications. The dehydrated oil had an API gravity of 25.6, classifying it as an intermediate to light crude oil. Furthermore, the low total acid number (TAN < 0.5 mg KOH g^{-1}) indicates that it is nonacidic. Together, these parameters provide a physicochemical characterization and can be associated with the molecular information obtained by FT-ICR MS. This highlights that despite its relatively light and nonacidic nature, the emulsion exhibits significant stability.

Table 1. Physicochemical Characterization of Emulsified Oil

properties	crude oil emulsion	methods
BSW (%. v $(v)^{-1}$)	54.4 (0.1)	ASTM D4007[33]
nonemulsified water or free water (%. v $(v)^{-1}$)	0.0	gravitational separation[19]
sediments (%. v $(v)^{-1}$)	0.40 (0.05)	ASTM D4007[33]
water content in oil after dehydration (%. v $(v)^{-1}$)	0.206 (0.0247)	Dehydration[19] ASTM D4377[34]
density at 20 °C (g $cm)^{-3}$	0.9000 (0.0002)	ASTM D5002[35]
API degree (°API)	25.6 (1)	ASTM D1250[36]
dynamic viscosity 40 °C (mPa·s)	34.949 (0.060)	ASTM D7042[37]
kinematic viscosity 40 °C $(mm^2\ s)^{-1}$	39.443 (0.065)	ASTM D7042[37]
point of maximum fluidity (°C)	9 (3)	ASTM D5853[38]
total acid number (TAN) (mg KOH $g)^{-1}$	0.389 (0.001)	ASTM D664[39]
total salinity index (TSI) (mg NaCl $kg)^{-1}$	3500 (78) 1,45,000 (7426)[a]	ASTM D6470[40]
pH in oil dehydration water at 25 °C	6.39 (0.24)	pHmetry
pH in oil wash water at 25 °C	6.5 (0.21)	pHmetry
surface tension (mN $m)^{-1}$	27.00 (0.70)	pendant drop
interfacial tension (mN m^{-1}) vs deionized water	6.74 (0.70)	pendant drop
interfacial tension (mN m^{-1}) vs formation water	4.26 (0.12)	pendant drop
droplet size distribution (DSD) (μm)	4.3 (0.4)	optical microscopy
saturated (S) (% m $m)^{-1}$	42.29 (0.16)	modified ASTM D2549[41,42]
aromatics (A) (% m $m)^{-1}$	24.98 (0.13)	modified ASTM D2549[41,42]
polars (P) (resins + asphaltenes) (% m $m)^{-1}$	32.72 (0.05)	modified ASTM D2549[41,42]

[a]Salt in the dehydration water.

Figure S1 presents detailed information on the composition using GC-FID profiles, providing a semiquantitative analysis. Bands corresponding to compounds with n-alkane carbon atoms ranging from n-C_7 to n-C_{30} were observed in emulsified crude oil, highlighting compounds in the range of n-C_{13} to n-C_{20}. The n-C_{17} and n-C_{18} have adjacent peaks known as pristane/C_{17} and phytane/C_{18} (n-C_{17}/Pr and n-C_{18}/Ph) that help in the identification of the other n-paraffins. These isoprenoid compounds are recognized for their resistance to biodegradation.[43,44]

3.2. Study of the Influence of Centrifugation Time. *3.2.1. Number of Assigned Compounds (ACs) and Distribution of M_w vs Centrifugation Time.* Analysis of the EPS (Figure S2j−p) and EPR (Figure S2c−i) fractions revealed the limitations of direct emulsion characterization, as the high aqueous and salt content caused ionic suppression in ESI(−) and loss of Gaussian spectral profiles after prolonged centrifugation (t > 60 min). To overcome these effects, interfacial material fractions (IMR and IMS) were isolated, producing more resolved mass spectra with reduced matrix interferences. IMR fractions (Figure 2c−h) showed an increase in the number of assigned compounds with the centrifugation time, while EPS exhibited the opposite trend. These results indicate a progressive transfer and enrichment of interfacially active species into the oil−water phases, while M_w remained essentially constant.

https://doi.org/10.1021/acs.energyfuels.5c03699
Energy Fuels 2025, 39, 18773−18790

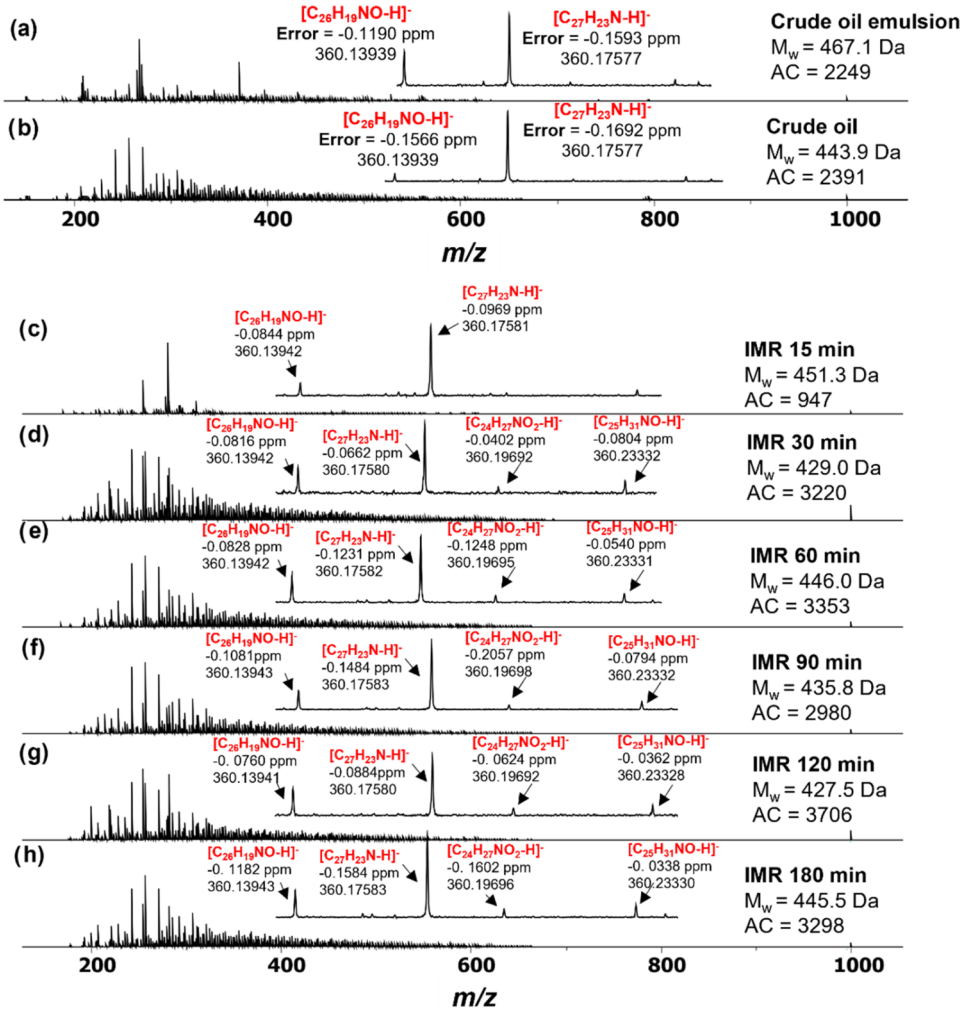

Figure 2. ESI(−) FT-ICR MS for the samples of (a) crude oil emulsion; (b) crude oil; and (c−h) IM of residue (IMR). The expansions show the experimental mass values, mass error (in ppm), and the molecular formula of species from the $NO_x[H]$ and $N[H]$ classes identified in the m/z range between 360.10 and 360.24.

Importantly, the IMR behavior confirms that centrifugation is not only a preparatory step but also a selective approach that enhances the detection of polar heteroatomic species associated with emulsion stability. This assertion is consistent with previous reports showing that interfacial isolates are chemically distinct from crude oil and enriched in oxygenated and sulfur-containing compounds,[27] containing a number of acidic species that contribute to emulsion stability,[26] and that functional isomers play a decisive role in interfacial activity.[22] Furthermore, the potential of these enriched fractions to act as natural demulsifiers has recently been recognized.[28] Thus, the present work aims to use centrifugation and understand how time and temperature parameters provide insight into how amphiphilic species migrate and accumulate at the oil−water interface, advancing the chemical understanding of emulsion stabilization beyond conventional mass analyses.

Figure 3 presents the distribution of M_w values for the major heteroatomic classes ($N_1[H]$, $O_1[H]$, $O_2[H]$, $N_1O_1[H]$, $N_1O_2[H]$, and $N_1O_3[H]$) as a function of centrifugation time. In the EPS fractions (Figure 3), a progressive decrease in M_w was observed, particularly for $O_2[H]$ and $N_1O_2[H]$, suggesting that lighter and more polar molecules preferentially migrate from the continuous oil phase toward the interfacial region. In contrast, the EPR fractions (Figure 3) showed nearly constant M_w values, an effect attributed to ion suppression caused by the high aqueous and saline content. Once salts and interferents were removed, the IMR fractions (Figure 3) revealed a systematic enrichment in higher M_w species, particularly for the $O_2[H]$ and $N_1O_3[H]$ classes, while $N_1[H]$ and $O_1[H]$ remained relatively unaffected. This selective enrichment demonstrates that centrifugation facilitates the transfer of acidic and mixed nitrogen oxygen species ($O_2[H]$, $N_1O_2[H]$, and $N_1O_3[H]$) into the interfacial material, reinforcing their role in emulsion stability.

A notable trend was observed for the $O_2[H]$ class (naphthenic acids, NAs). At short centrifugation times (t = 15 min), low M_w NAs (<450 Da) dominated all fractions, consistent with their high polarity and known interfacial activity. Their strong presence in IMR highlights their preferential association with the interfacial layer, corroborating previous study that identified NAs as key contributors to emulsion stabilization.[53] Moreover, the detection of $N_1O_3[H]$ compounds exclusively in the IMR and IMS fractions but not in EPR or EPS suggests a lower migration rate of these species and a stronger affinity for the dehydrated interfacial layer. This may reflect a substitution mechanism in which more active amphiphile compounds displace weaker ones at the droplet

https://doi.org/10.1021/acs.energyfuels.5c03699
Energy Fuels 2025, 39, 18773−18790

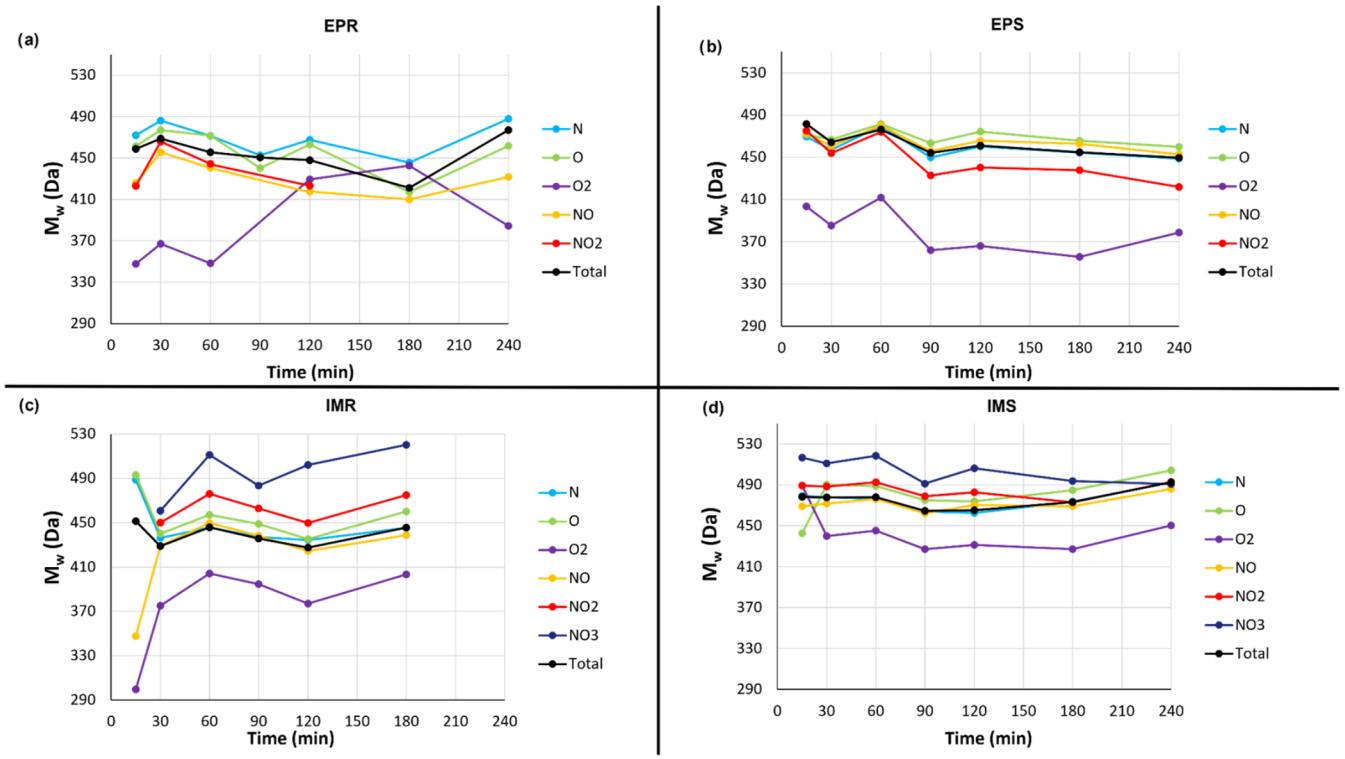

Figure 3. Distribution of M_w for the $N_1[H]$, $O_1[H]$, $O_2[H]$, $N_1O_1[H]$, $N_1O_2[H]$, and $N_1O_3[H]$ classes obtained from the ESI(−)FT-ICR data for the emulsified crude oil and its fractions ((a) (EPR), (b) (EPS), (c) (IMR), and (d) (IMS)) as a function of centrifugation time.

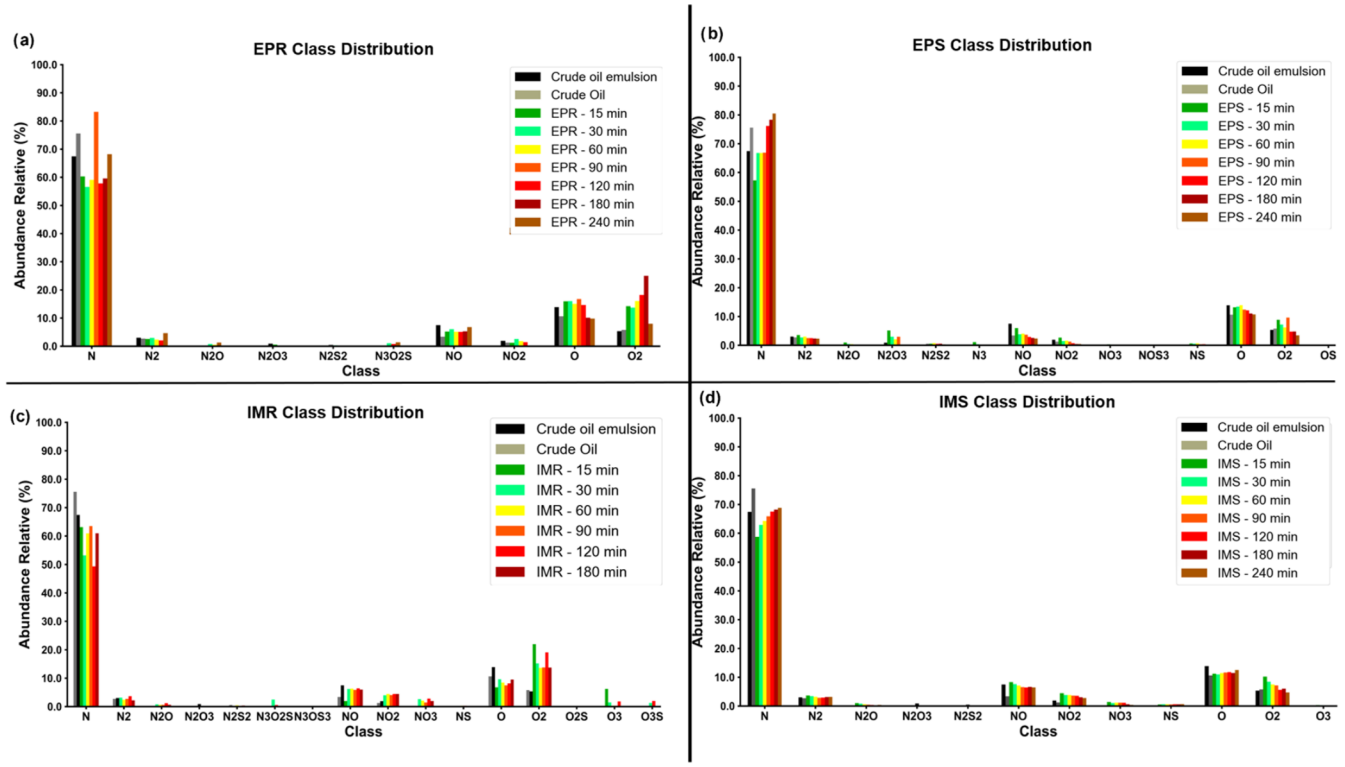

Figure 4. Class distribution by relative abundance of crude oil emulsion samples and their fractions: (a) EPR, (b) EPS, (c) IMR, and (d) IMS as a function of centrifugation time obtained from ESI(−) FT-ICR MS data.

interface, as proposed for NAs competing with asphaltenes in previous reports.

Interestingly, the absence of $N_1O_2[H]$ species in IMR at short centrifugation times, despite their presence in crude and emulsified oils, suggests either a loss during Dean−Stark extraction or solubilization into the aqueous phase. This indicates that specific oxygenated nitrogen compounds may partition away from the interfacial layer, depending on their

https://doi.org/10.1021/acs.energyfuels.5c03699
Energy Fuels 2025, 39, 18773−18790

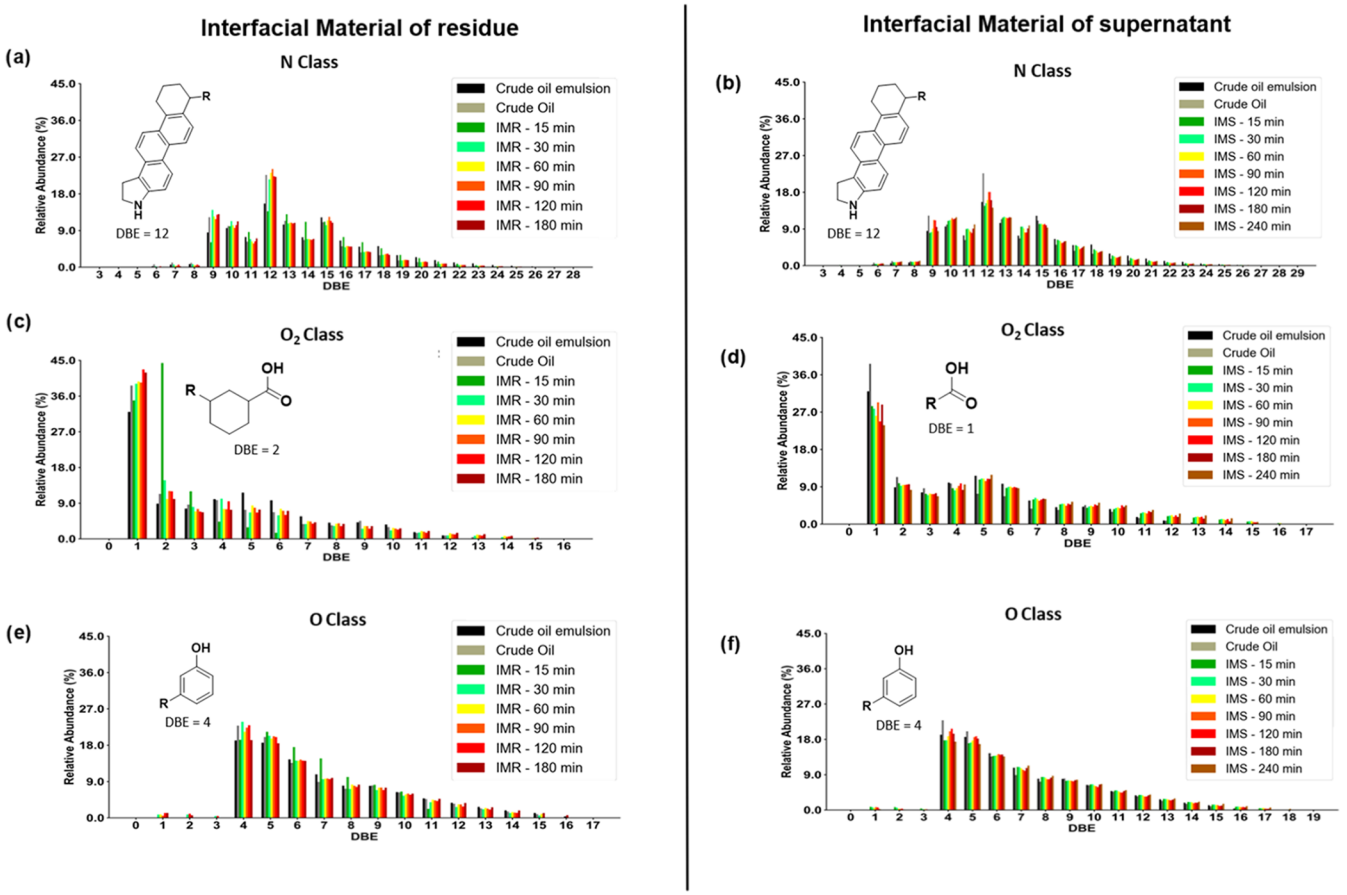

Figure 5. Distribution of DBEs vs. relative abundance for the IMR and IMS fraction samples of the emulsified oil as a function of the centrifugation time study for the classes: $N_1[H]$ (a, b), $O_2[H]$ (c, d), and $O_1[H]$ (e, f).

polarity and ionizable functional groups. Collectively, these findings demonstrate that centrifugation not only separates phases but also provides a dynamic framework to monitor how amphiphilic species migrate, concentrate, and stabilize the water−oil interface, offering molecular-level evidence for mechanisms long hypothesized in emulsion stability.

3.2.2. Abundance of Classes vs Centrifugation Time. Figure 4 presents the relative abundance of heteroatom classes assigned from the ESI(−) FT-ICR MS data of the crude oil emulsion and its fractions. Nitrogen-containing species ($N_1[H]$) dominated all samples, confirming their widespread presence also at the oil−water interface. Oxygenated classes displayed distinct behaviors: $O_2[H]$ compounds were particularly enriched in IMR, while $O_1[H]$ species were more prominent in EPS and IMS. The competition between $O_1[H]$ and $O_2[H]$ in EPR fractions suggests dynamic partitioning, with naphthenic acids ($O_2[H]$) progressively migrating toward the IMR fraction. This observation provides evidence that low molecular weight naphthenic acids exert a direct effect on interfacial tension, while high molecular weight species stabilize emulsions through secondary mechanisms.[53] In contrast, the weaker polarity and nonionic nature of the $O_1[H]$ species likely reduce their affinity for the aqueous phase, favoring their persistence in EPS and IMS. Overall, these results highlight that centrifugation-based isolation not only separates phases but also discriminates between molecular classes according to their interfacial activity, providing mechanistic insight into how nitrogen- and oxygen-containing species contribute to emulsion stability, in addition to considering the oil as a whole.

The heteroatom class distributions highlight the selective enrichment of amphiphilic species at the oil−water interface under centrifugation. The EPR fractions contained mixed nitrogen, oxygen, and sulfur species ($N_2O_1[H]$, $N_2O_3[H]$, $N_3O_2S_1[H]$) not detected in the crude oil or emulsion, indicating the formation or preferential retention of these classes in the unresolved emulsion residue. A slight decrease in the level of $O_2[H]$ with time in EPR suggests progressive transfer of NAs toward the interfacial layer. In contrast, IMR fractions exhibited a marked enrichment of polar and mixed classes ($N_2O_1[H]$, $N_1O_2[H]$, and $O_2[H]$) and the appearance of new heteroatomic groups ($O_3[H]$, $N_1O_3[H]$, and $O_3S_1[H]$), while EPS and IMS fractions showed a corresponding reduction. This compositional shift confirms the migration of oxygenated and nitrogen oxygen species to the interface, consistent with their higher polarity and interfacial activity. Interestingly, the persistence and increasing abundance of the $N_1[H]$ class in EPS and IMS with centrifugation time indicate that these species remain largely bulk-associated and play a minor role in interfacial stabilization compared with oxygenated and mixed heteroatomic compounds. Overall, these trends demonstrate that centrifugation selectively drives the accumulation of interfacially active classes into IMR, providing molecular-level evidence of their role in emulsion stability.

3.2.3. DBE vs Centrifugation Time. Figure 5 shows that the DBE distributions of the major heteroatom classes provide

https://doi.org/10.1021/acs.energyfuels.5c03699
Energy Fuels 2025, 39, 18773−18790

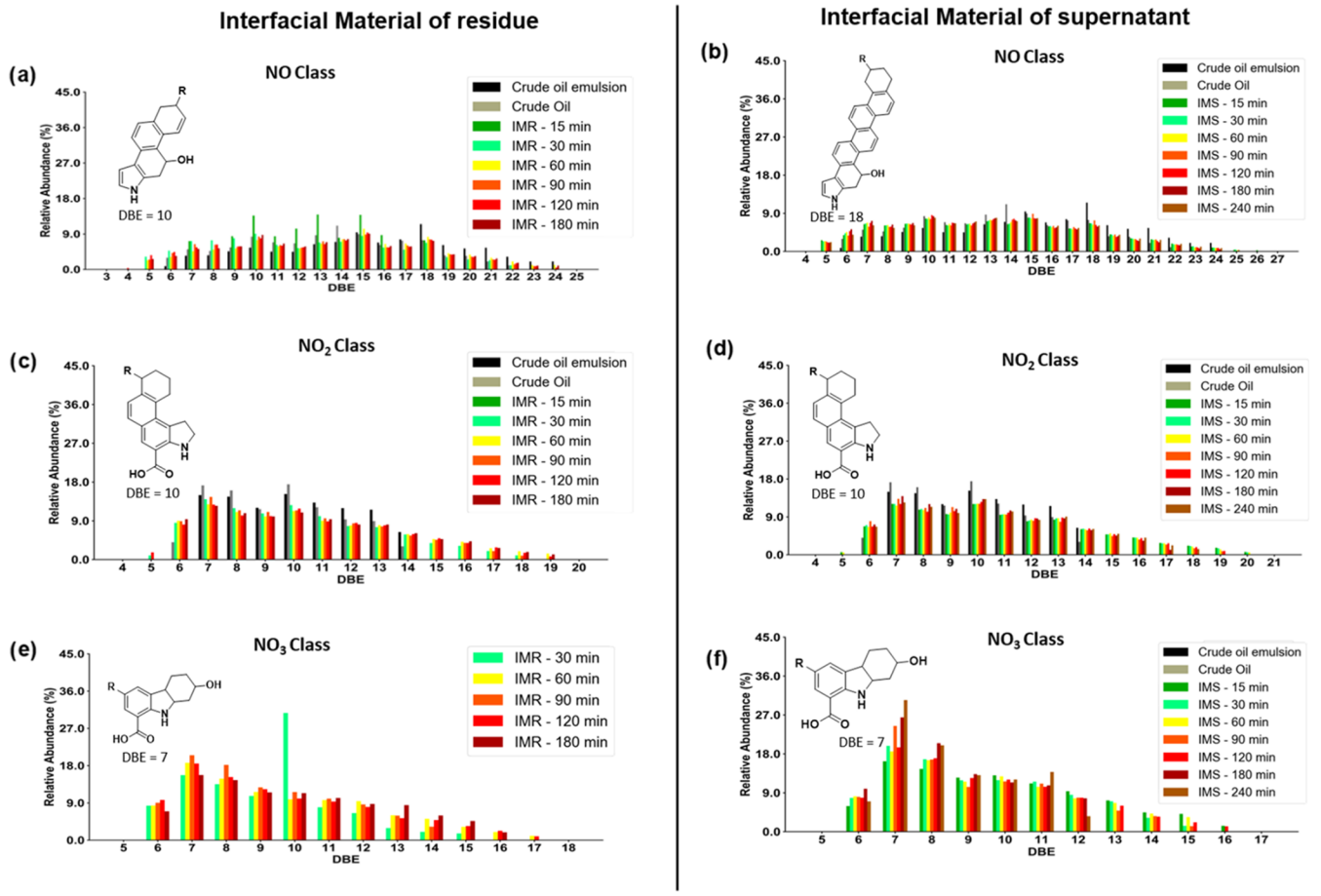

Figure 6. Distribution of DBE vs. relative abundance for the classes $N_1O_1[H]$ (a, b), N_1O_2 [H] (c, d), and N_1O_3 [H] (e, f) for the emulsified oil and the IMR and IMS fractions.

molecular evidence of selective enrichment of aromatic and oxygenated compounds at the oil−water interface.

In both IMR and IMS, $N_1[H]$ species were dominated by benzocarbazoles (DBE 12) and dibenzocarbazoles (DBE 15),[54−58] indicating that highly aromatic nitrogen compounds are preferentially concentrated in the interfacial material. The $O_2[H]$ class, corresponding to naphthenic acids (DBE 1−11), exhibited two distinct trends: linear carboxylic acids (DBE = 1) were most abundant at short centrifugation times, suggesting rapid migration to the interface, while polyaromatic acids (DBE > 5) accumulated more gradually, reflecting their slower transfer and stronger interfacial association.[59] In IMS, the relative abundance of low-DBE acids was reduced, reinforcing that these compounds preferentially partition into the IMR.

Phenolic-like $O_1[H]$ species[60] were detected over a broad DBE range (4−16), with enrichment at DBE = 4−6 in IMR, consistent with the accumulation of hydroxylated aromatics at the interface. Notably, nonphenolic species (DBE = 1−3), absent from crude oil and emulsion spectra, appeared exclusively in IMR and IMS and increased with centrifugation time. Their presence indicates that centrifugation enhances the detection of amphiphilic compounds otherwise suppressed by matrix effects in the mass spectrometry analysis. Collectively, these results confirm that centrifugation selectively concentrates aromatic N compounds, naphthenic acids, and phenolic species at the emulsion interface, demonstrating their key role in lowering the interfacial tension and strengthening the interfacial films.

Figure 6 analysis of $N_1O_1[H]$, $N_1O_2[H]$, and $N_1O_3[H]$ classes (DBE ranges of 5−24, 5−19, and 6−17, respectively) revealed clear differences in their interfacial behavior.

In IMR, both $N_1O_2[H]$ and $N_1O_3[H]$ species were progressively enriched at high DBE values (>11−12), consistent with the accumulation of highly aromatic and heteroatom-rich compounds at the interface, while $N_1O_1[H]$ remained relatively constant. In contrast, the $O_2[H]$ species, which include low M_w carboxylic acids, migrated more rapidly due to their polarity and mobility, whereas the more unsaturated and aromatic $N_1O_2[H]$ and $N_1O_3[H]$ classes exhibited stronger adsorption at the interface. This behavior is consistent with the well-established role of acidic and polyaromatic compounds in emulsion stabilization, where ionic groups promote strong interactions with water droplets and heavier, polyunsaturated molecules contribute to colloidal aggregation, similar to asphaltenes and resins. Notably, the $N_1O_3[H]$ class (DBE ≈ 10) contains both acidic and phenolic functionalities, suggesting that these multifunctional species act synergistically to reduce interfacial tension and reinforce interfacial films. Collectively, these findings confirm that both low M_w acids and high DBE heteroatomic species cooperate in stabilizing emulsions: the former by lowering interfacial tension and the latter by enhancing the rigidity of the interfacial layer.[6,53]

3.2.4. Number of Carbons (#C) vs Centrifugation Time. Figure 7 shows the carbon number distributions (#C) of the $O_2[H]$ species that provide additional evidence for the

https://doi.org/10.1021/acs.energyfuels.5c03699
Energy Fuels 2025, 39, 18773−18790

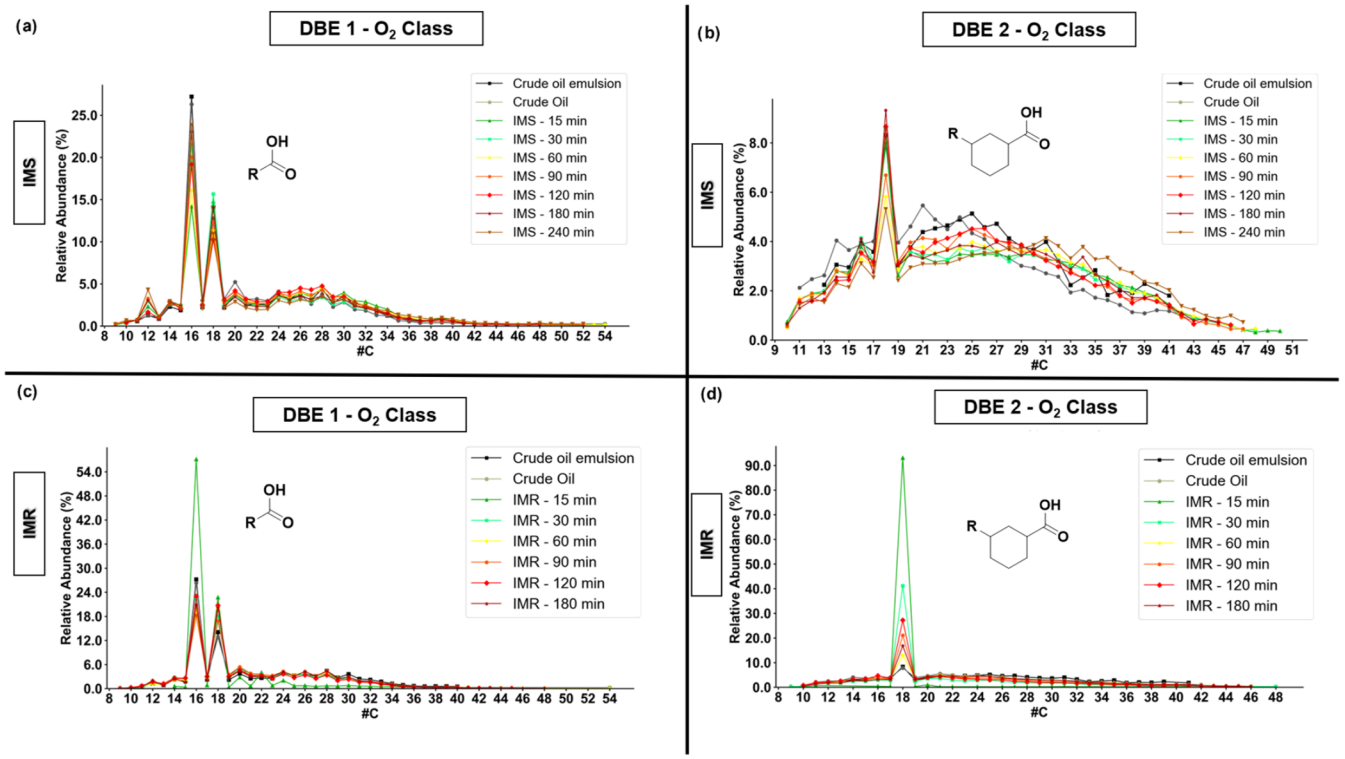

Figure 7. Distribution of *#C* by relative abundance for the O_2[H] class referring to DBEs = 1 and 2 for the IMR (a, c) and (b, d) IMS fractions as a function of centrifugation time.

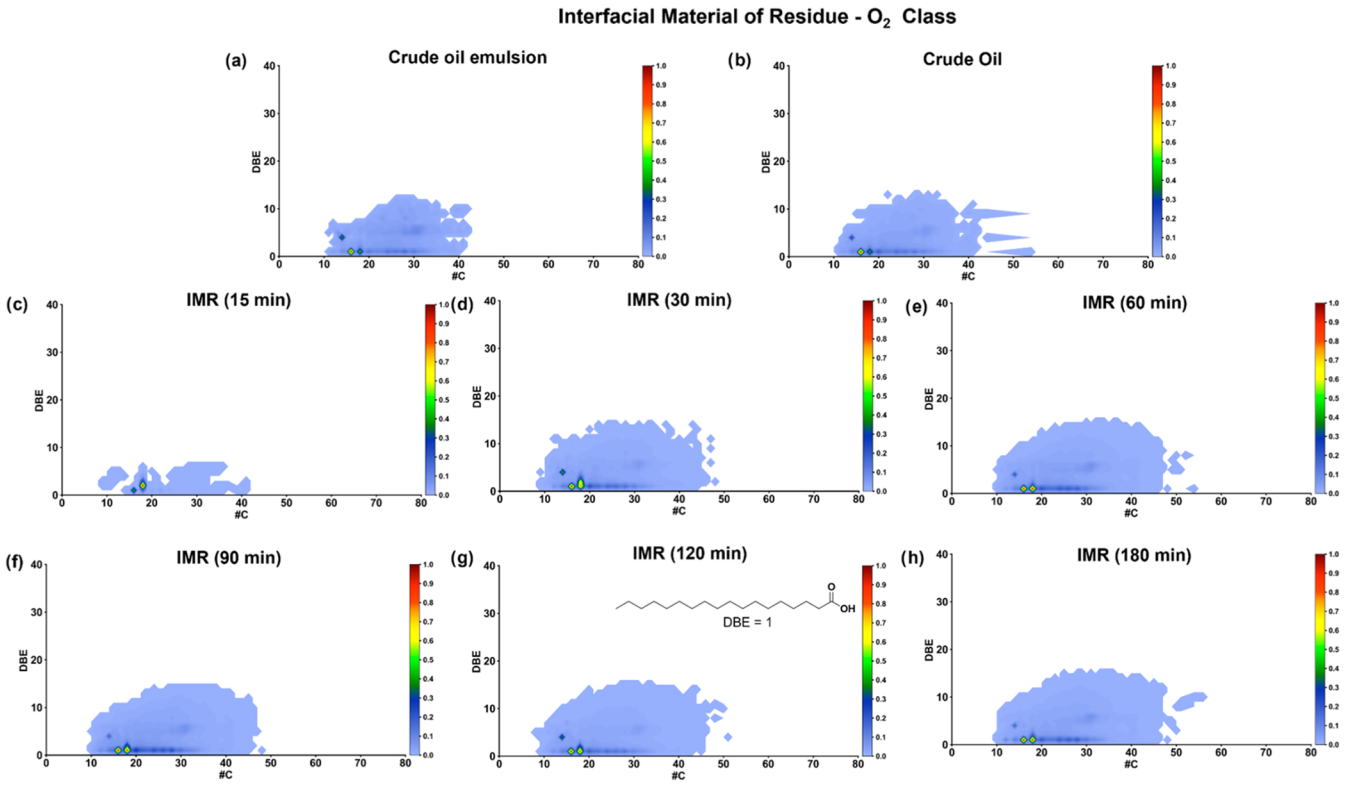

Figure 8. Plots of DBE vs. *#C* for the O_2 class species [H] of the (a) crude oil emulsion and (b) crude oil and its IMR fractions as a function of centrifugation time: (c) 15 min, (d) 30 min, (e) 60 min, (f) 90 min, (g) 120 min, and (h) 180 min.

selective enrichment of NAs at the oil−water interface. Linear acids (DBE = 1) dominated both IMR and IMS, spanning wide *#C* ranges (C_9−C_{48-54}) but showing a maximum relative abundance at C_{16}−C_{18}, consistent with the prevalence of medium-chain carboxylic acids at the interface. Monocyclic acids (DBE = 2) exhibited similar maxima at C_{16}−C_{18}, which

https://doi.org/10.1021/acs.energyfuels.5c03699
Energy Fuels 2025, 39, 18773−18790

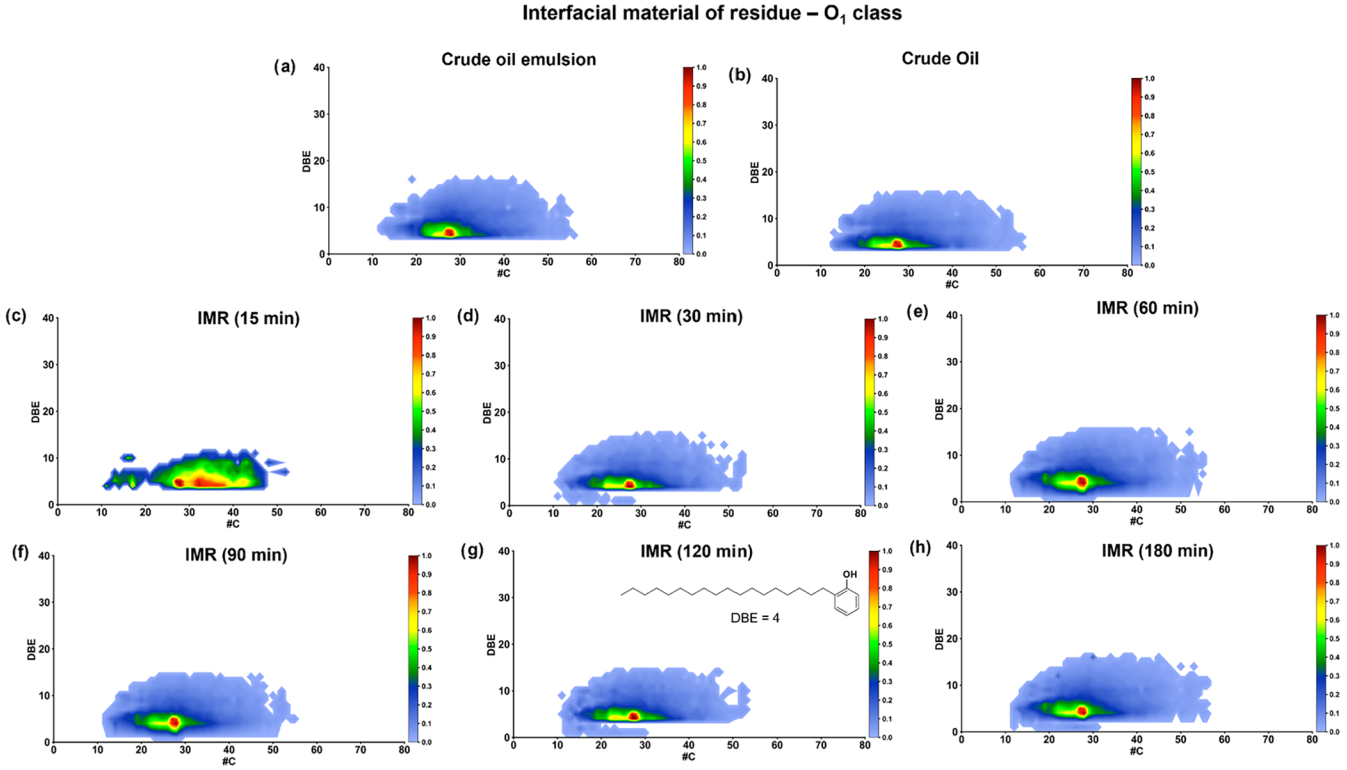

Figure 9. Plots of DBE vs. #*C* for class O_1 species [H] of the (a) crude oil emulsion and (b) crude oil and its IMR fractions obtained as a function of centrifugation time: (c) 15 min, (d) 30 min, (e) 60 min, (f) 90 min, (g) 120 min, and (h) 180 min.

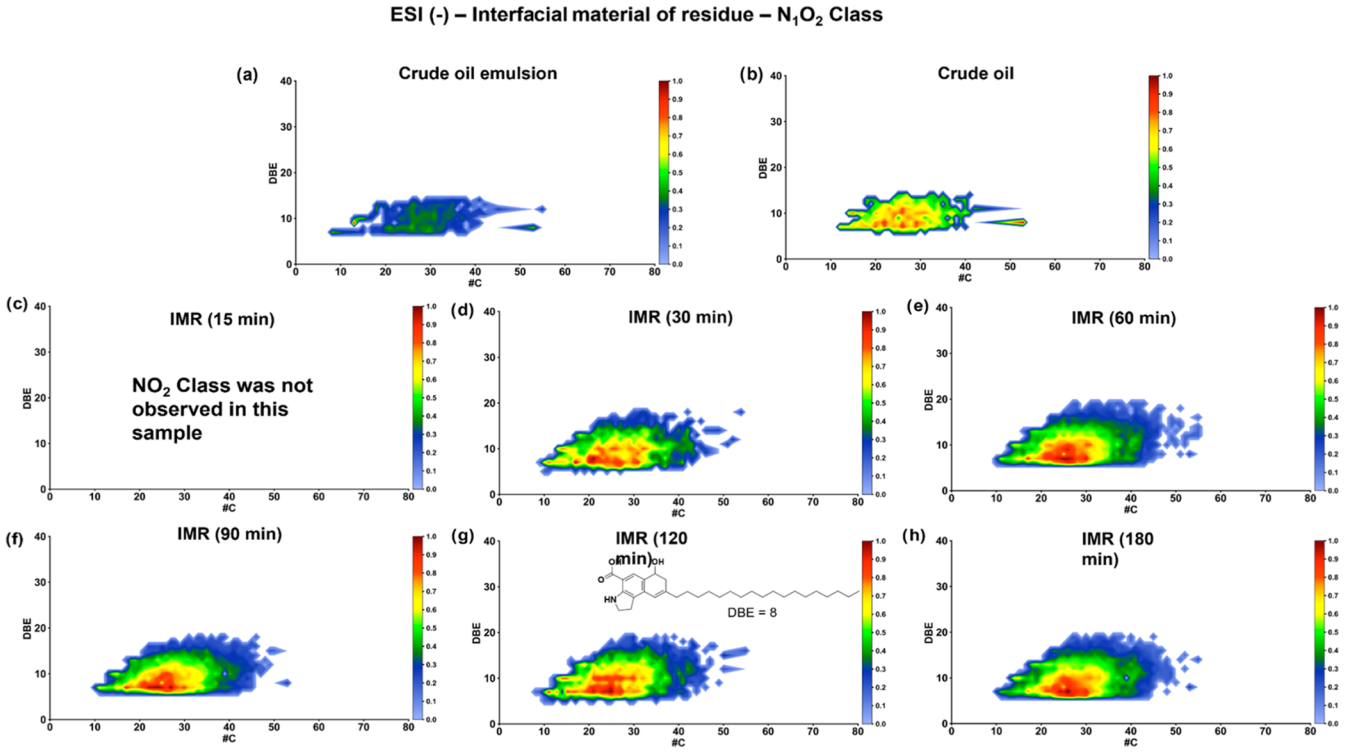

Figure 10. Plots of DBE vs. #*C* for N_1O_2[H] class species of the (a) crude oil emulsion and (b) crude oil and its IMR fractions as a function of centrifugation time: (c) 15 min, (d) 30 min, (e) 60 min, (f) 90 min, (g) 120 min, and (h) 180 min.

correspond to fatty acids such as palmitic and stearic acid, reported as possible contaminants in petroleum systems.[61] Nevertheless, the persistence of these species across both IMR and IMS fractions, with increasing relative abundance of C_{18} compounds at early centrifugation times (15−30 min), suggests that amphiphilic carboxylic acids are rapidly mobilized toward the interfacial layer. This behavior highlights the dual role of O_2[H] species: lower-carbon, linear acids migrate

https://doi.org/10.1021/acs.energyfuels.5c03699
Energy Fuels 2025, 39, 18773−18790

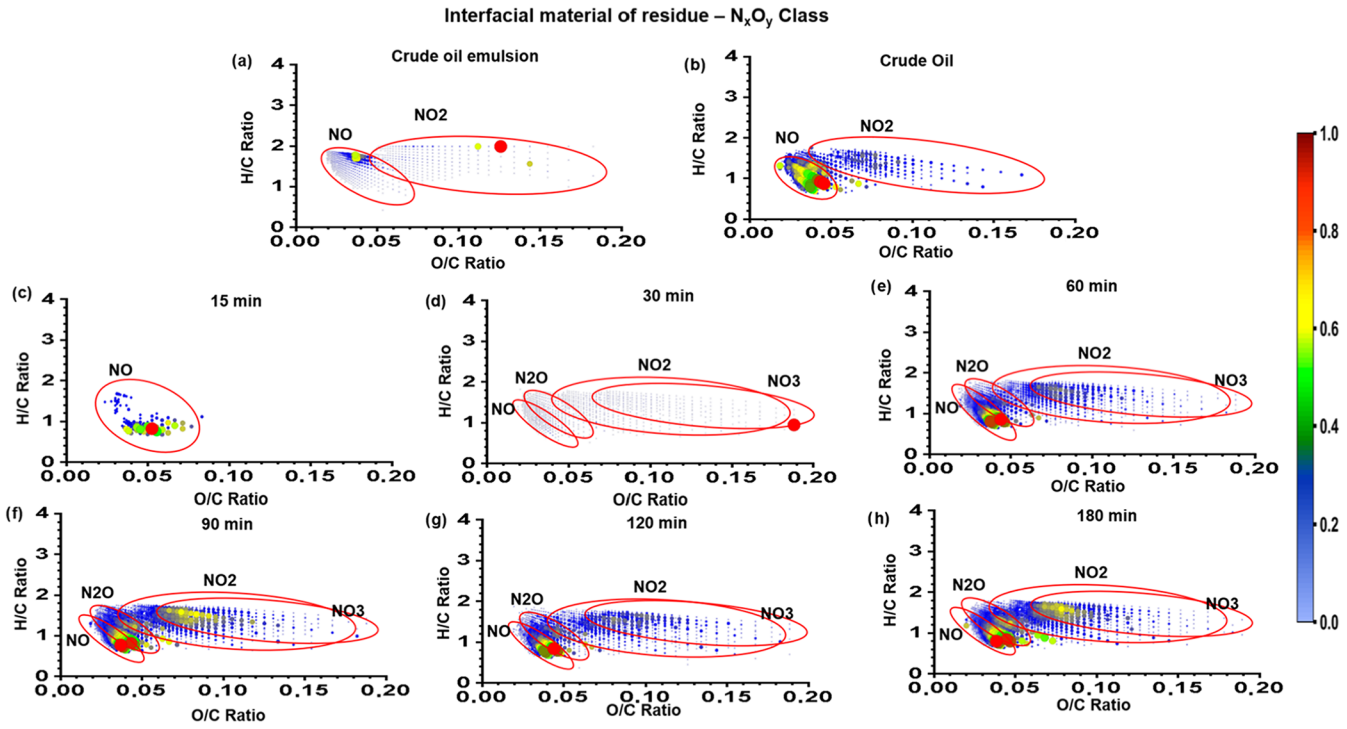

Figure 11. Van Krevelen diagrams for $N_XO_Y[H]$ species of the crude oil: (a) crude oil emulsion and (b) crude oil and their IMR fractions as a function of centrifugation time: (c) 15 min, (d) 30 min, (e) 60 min, (f) 90 min, (g) 120 min, and (h) 180 min.

quickly and contribute to interfacial tension reduction, while cyclic and higher-carbon members accumulate more slowly, potentially reinforcing interfacial stability.

3.2.5. DBE vs #C Ratio as a Function of Centrifugation Time. The DBE is vs. *#C* graph for $O_2[H]$ class compares the crude oil emulsion and crude oil samples with the IMR samples as a function of centrifugation time, Figure 8. Table S2 of the Supporting Information shows the range of *#C* and DBE observed.

The comparison of IMR fractions across centrifugation times (15 and 240 min) demonstrates that extended separation increases the chemical diversity of interfacial naphthenic acids, with the *#C* range expanding from C_9−C_{41} to C_9−C_{58} and DBE values from 0−8 to 0−18. At intermediate times (30−180 min), the most abundant species remained concentrated at C_{16}−C_{18} with DBE = 1, consistent with saturated fatty acids, such as palmitic and stearic acids. The progressive enrichment of higher-carbon, low-DBE species at longer centrifugation times suggests a preferential migration of saturated carboxylic acids toward the interfacial layer, reinforcing their role as dominant contributors to interfacial activity. This behavior corroborates previous reports that identified saturated fatty acids, phenols, carbazoles, and indoles as interfacial components in petroleum and related organic matrices.[62−64] Furthermore, $O_2[H]$ acids with a DBE of 1 were consistently enriched in IMR, confirming their strong partitioning from maltene and asphaltene fractions to the interface. For species with DBE < 10, our data suggest the presence of up to nine conjugated monocyclic rings,[61−64] indicating that more complex aromatic structures coexist with low M_w acids to stabilize the interface. Collectively, these results demonstrate that centrifugation does not merely concentrate pre-existing acids but dynamically modulates the enrichment of both saturated and aromatic $O_2[H]$ species, providing mechanistic evidence of their role in interfacial film formation.

Figure 9 shows the DBE distribution for the $O_1[H]$ class. It reveals an enrichment of phenolic-like species (DBEs 4−5) in IMR samples from 15 to 180 min. This suggests that polar functionalities, such as alcohols and phenols, progressively migrate to the interface. However, alcohols are poorly ionized under ESI(−) conditions.[51] After 30 min, additional low-abundance compounds with DBE < 4 were detected, which may correspond to aldehydes, ethers, and ketones. This indicates that longer centrifugation times favor a broader diversity of oxygenated functionalities. The $N_1O_2[H]$ class (Figure 10) showed an increase in both the DBE and carbon number ranges with longer centrifugation times. This reinforces the selective accumulation of highly aromatic and polar mixed N/O species at the interface. These observations are consistent with the enhanced chemical diversity in the interfacial material. However, we acknowledge that using only ESI(−) mode may underestimate neutral oxygenates, such as aldehydes and ketones, which are more efficiently detected by APPI(+) or derivatized ESI(+) approaches.[65] Although APPI is more effective at ionizing neutral oxygenates (e.g., aldehydes and ketones) that are under-represented in ESI, both techniques consistently show an enrichment of $O_2[H]$ acids and mixed N/O classes in the interfacial fractions. This agreement indicates that the observed compositional trends are not side effects of the ionization factor but reflect unique interfacial processes.

Unlike the $O_2[H]$ class, which displayed relatively narrow distributions (Table S2), the $N_1O_2[H]$ class (Figure 10) exhibited broader ranges (*#C* = 12−40, DBE = 5−15), indicating the selective migration of more aromatic and polar molecules to the emulsion interface. A similar pattern was observed for the $N_1O_3[H]$ class (Figure S5), with distributions extending from *#C* = 20−42 and DBE = 5−12, especially with longer centrifugation times (60−120 min). The broadening of the *#C* and DBE ranges with centrifugation reflects the

https://doi.org/10.1021/acs.energyfuels.5c03699
Energy Fuels 2025, 39, 18773−18790

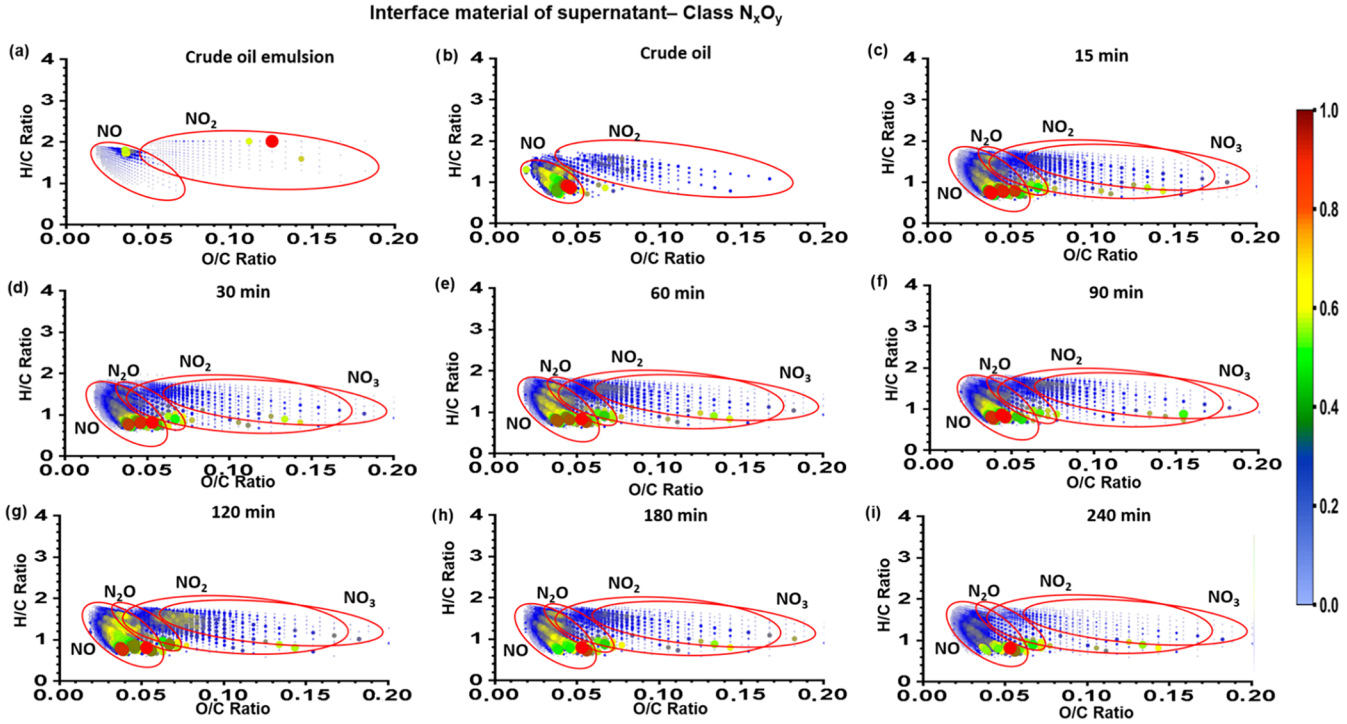

Figure 12. Van Krevelen diagrams for $N_XO_Y[H]$ species of the crude oil: (a) crude oil emulsion and (b) crude oil and their IMS fractions as a function of centrifugation time: (c) 15 min, (d) 30 min, (e) 60 min, (f) 90 min, (g) 120 min, and (h) 180 min.

progressive enrichment of multifunctional nitrogen−oxygen species that likely interact strongly with the interfacial film through a combination of polarity, aromaticity, and hydrogen-bonding capacity.

These results emphasize that prolonged centrifugation not only concentrates classical amphiphilic acids but also increases the chemical diversity of the interfacial material by mobilizing highly aromatic heteroatomic compounds. This diversity is to be expected since the composition of interfacial films is inherently heterogeneous and varies with droplet surface area, adsorption kinetics, the availability of amphiphiles, and the solubility of individual species in the surrounding medium.[21,32] Together, this evidence highlights molecular-level information that centrifugation captures the dynamic and heterogeneous nature of interfacial material formation, which extends beyond the static compositional profiles obtained from mass spectrometry analyses.

3.2.6. Van Krevelen Diagram vs Centrifugation Time. Van Krevelen's analysis of $N_xO_y[H]$ species[66,67] further highlights the selective enrichment of mixed nitrogen−oxygen compounds at the emulsion interface. Figure 11 presents the IMR fraction. Note that the $N_1O_2[H]$ class was absent after 15 min but increased steadily thereafter. The $N_1O_3[H]$ species emerged after 30 min. These trends are consistent with the DBE vs #C plots and indicate the progressive migration and accumulation of multifunctional heteroatomic species in the interfacial residue. In contrast, IMS (Figure 12) and mass fractions retained higher relative abundances of $N_xO_y[H]$ species during the early stages of centrifugation (15−60 min), suggesting that these compounds initially partition into the dispersed aqueous phase before concentrating at the interfacial layer. Together, these results show that centrifugation captures the dynamic partitioning of the nitrogen and oxygen classes.

3.3. Study of the Influence of Centrifugation Temperature. *3.3.1. Influence of Centrifugation Temperature on AC and M_w.* Figure 13 shows how the centrifugation temperature significantly affects the accumulation of interfacial material in the IMR fractions. As the temperature increased, so did the number of assigned compounds (ACs) in the IMR fraction. The highest number of ACs was observed at 60 °C (3706), and the lowest number was observed at 20 °C (1179). This trend underscores the importance of temperature in facilitating the migration of interfacially active species into the unresolved phase. Compounds that were previously suppressed in the EPR fraction only became detectable after water was removed. The temperature-dependent increase in AC in the IMR fraction is consistent with the findings of earlier studies suggesting that higher temperatures reduce emulsion viscosity, thereby promoting the migration of suspended species to the interfacial phase.[68−70]

Conversely, a significant reduction in AC was observed in the EPR fractions at higher temperatures (EPR 20 °C: 2,691; EPR 60 °C: 1,875), likely due to the ion suppression effect discussed in Section 3.2. Removing water and salts from the EPR and EPS phases at higher temperatures improves the ionization efficiency, enhancing the detection of polar and amphiphilic species in the IMR and IMS fractions. This temperature-driven dynamic illustrates how centrifugation separates phases and modulates the partitioning of interfacial species.

3.3.2. Abundance of Classes vs Centrifugation Temperature. The influence of the centrifugation temperature on the chemical profile of the interfacial material revealed distinct behaviors across the fractions. IMS showed relatively little variation in the number of assigned compounds, whereas IMR displayed a consistent increase and reached higher AC values than the crude oil, emulsified oil, and emulsified crude oil. For EPR, increasing the temperature reduced M_w values across all classes, reflecting ion suppression and the loss of polar compounds to the aqueous/saline phase. Conversely, the

https://doi.org/10.1021/acs.energyfuels.5c03699
Energy Fuels 2025, 39, 18773−18790

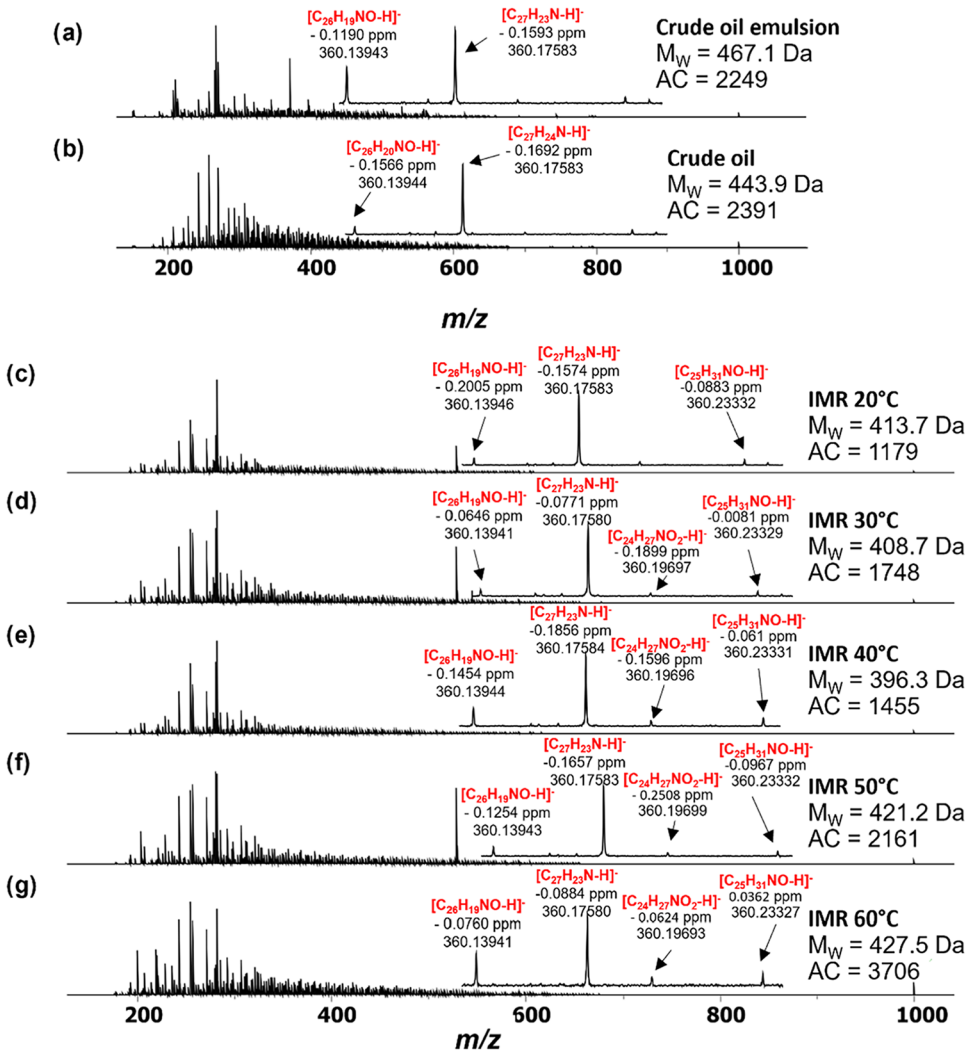

Figure 13. Mass spectra of the (a) crude oil emulsion and (b) crude oil and its (c–g) IMR as a function of centrifugation temperature acquired by ESI(−) FT-ICR MS.

IMR exhibited higher M_w values with increasing temperature, particularly for the corresponding regions $O_2[H]$, $N_1O_1[H]$, and $N_1O_2[H]$. This indicates that elevated temperatures facilitate the migration of heavier, more polar amphiphiles to the interfacial layer.

Figure S9 shows that the class distributions confirmed that $N_1[H]$ dominated all samples, followed by those of $O_1[H]$ and $O_2[H]$, consistent with the time-dependent study. However, temperature exerted a stronger influence on $O_2[H]$ (naphthenic acids), which increased steadily in both EPR and IMR. This suggests that these acids preferentially partition into the unresolved phase at higher temperatures. Conversely, other heteroatomic classes (e.g., $N_1O_3[H]$, $O_3[H]$, and $N_1S_1[H]$) appeared in the IMR but did not increase in relative abundance with temperature. This highlights that temperature enhances the migration of simpler oxygenated acids rather than complex mixed species. Overall, these results demonstrate that, while temperature modulates the mobility of naphthenic acids and certain polar compounds during centrifugation, its effect on highly aromatic or multifunctional species is less pronounced.

3.3.3. DBEs vs Temperature Influence. Figure S11 of the Supporting Information shows that the DBE distributions confirm that the enrichment of oxygenated and mixed heteroatomic species at the oil/water interface is selectively modulated by centrifugation parameters. For most classes ($N_1[H]$, $O_2[H]$, and $O_1[H]$), the DBE profiles remained constant. However, for $O_1[H]$, DBE species (1–3) emerged in IMR and IMS. This is consistent with the migration of aldehydes, ketones, and ether derivatives to the interfacial material. Within the $O_2[H]$ class, both DBE naphthenic acids (1–2) and higher-DBE (12–14) naphthenic acids were enriched in IMR and IMS. This reinforces their dual role as rapidly migrating acids that lower interfacial tension and as more aromatic acids that contribute to film rigidity.

Mixed nitrogen oxygen classes (Figure S12) exhibited similar trends under time and temperature variations. $N_1O_2[H]$ species with DBEs of 12–19 increased systematically in IMR as the temperature of the centrifugation increased, while $N_1O_3[H]$ compounds were detected only at 60 °C, spanning DBE values from 6 to 17. These results demonstrate that, similar to longer centrifugation times, elevated temperatures promote the migration and accumulation of strongly polar, aromatic, multifunctional species at the interface. The consistency between time- and temperature-dependent experiments highlights that centrifugation selectively enriches oxygenated and N/O-containing amphiphile compounds in

https://doi.org/10.1021/acs.energyfuels.5c03699
Energy Fuels 2025, 39, 18773–18790

Table 2. Trend in Relative Abundance of Classes as a Function of Increasing Centrifugation Time and Temperature for EPR, EPS, IMR, and IMS Fractions[a]

		classes												
factors	samples	$N_1[H]$	$N_2[H]$	$O_1[H]$	$O_2[H]$	$O_3[H]$	$N_1O_1[H]$	$N_1O_2[H]$	$N_1O_3[H]$	$N_2O_1[H]$	$N_1S_1[H]$	$N_2S_2[H]$	$N_3O_2S[H]$	$O_3S_1[H]$
time	EPR	xx	+	−	+	nsd	+	−	nsd	+	nsd	xx	xx	nsd
	EPS	+	−	−	−	nsd	−	−	nsd	xx	−	xx	nsd	nsd
	IMR	xx	−	xx	+	+	xx	+	+	+	nsd	xx	−	+
	IMS	+	−	+	+	nsd	−	+	+	+	+	xx	nsd	nsd
temperature	EPR	−	−	xx	+	nsd	xx	+	nsd	−	nsd	nsd	xx	nsd
	EPS	xx	xx	xx	+	nsd	xx	xx	nsd	nsd	xx	xx	nsd	nsd
	IMR	−	+	−	+	−	+	+	+	xx	nsd	xx	−	xx
	IMS	xx	xx	xx	xx	nsd	−	+	+	xx	xx	xx	nsd	nsd

[a]+: tends to increase; −: tends to decrease; nsd: no significant detection; xx: no defined trend.

the interfacial material. This provides insight into the molecular basis of emulsion stability.

3.3.4. #C vs Temperature Influence. Temperature also modulated the partitioning of naphthenic acids (Figure S13) into the interfacial fractions. Linear (DBE = 1) and cyclic (DBE = 2) NAs, which are dominated by C_{16} and C_{18} compounds, were consistently enriched in the IMR and IMS, indicating the rapid migration of medium-chain carboxylic acids to the interface. Although some of these species may correspond to fatty acid contaminants,[61,71] their persistence under all conditions suggests that amphiphilic carboxylates play a key role in interfacial activity. In addition to NAs, the $N_1O_3[H]$ class with DBE ≈ 15 also exhibited temperature-dependent migration. The *#C* broadened from C_{19}−C_{31} at 20 °C to C_9−C_{42} at 60 °C. This expansion reflects the increased mobility of N/O-containing multifunctional aromatic species at elevated temperatures and reinforces the idea that temperature facilitates the enrichment of simple acids and complex heteroatomic compounds in interfacial material. They thus demonstrate that centrifugation at higher temperatures not only increases the abundance of interfacially active species but also expands their chemical diversity, thus strengthening the molecular basis for emulsion stability.

3.3.5. DBE and #C vs Centrifuge Temperature for Class O_2[H]. The effect of the centrifugation temperature on DBE vs. *#C* (Figure S16) reveals a broader chemical diversity of the interfacial material at elevated temperatures. For the $O_2[H]$ species, the IMR fractions exhibited a progressive widening of the *#C* value compared to the crude and emulsified oils. The maximum was centered on C_{10}−C_{32} (DBE = 1), which indicates an enhanced detection of naphthenic acids at higher temperatures. Similar behavior was observed for the $N_1O_2[H]$ and $O_1[H]$ classes. The range of detected compounds expanded significantly at 60 °C (up to DBE = 20 and C_{50}−C_{59}), suggesting that higher temperatures promote the migration of more aromatic and polar amphiphiles into the interfacial phase. In contrast, $N_1O_3[H]$ species were detected only under high-temperature conditions, which is consistent with their stronger adsorption and lower mobility at the interface.

The intensity of the $N_1O_2[H]$ species increased markedly in the IMR at 60 °C. The IMS fractions exhibited greater aromaticity with increasing temperature, as reflected by lower H/C ratios.

3.3.6. Van Krevelen Diagram vs Centrifuge Temperature for Class N_xO_y[H]. Figures S20 and S21 of the Supporting Information show that Van Krevelen analysis confirmed that increasing the temperature of centrifugation enhances the migration of mixed nitrogen oxygen species to the interfacial layer. In the IMR, $N_1O_2[H]$ compounds became progressively more abundant at higher temperatures, indicating that these polar amphiphiles migrate faster at elevated temperatures. In IMS, higher aromaticity was observed at 60 °C, as reflected by lower H/C ratios. This is consistent with the preferential enrichment of aromatic, oxygenated, and nitrogen−oxygen species at the interface.

Table 2 shows that the classes most sensitive to centrifugation parameters were $N_1[H]$, $N_2[H]$, $O_1[H]$, $O_2[H]$, $O_3[H]$, $N_1O_1[H]$, $N_1O_2[H]$, $N_1O_3[H]$, and $N_2O_1[H]$. In contrast, sulfur-containing species such as $N_1S_1[H]$, $N_2S_2[H]$, and $O_3S_1[H]$ showed no consistent response. Notably, the abundance of $N_3O_2S_1[H]$ decreased with increasing time and temperature, contrary to previous reports which described sulfoxide-containing classes (e.g., O_4S) as key contributors to emulsion stability due to their ability to form hydrogen bonds and interact with asphaltenes to produce stable interfacial films.[60,72,75] The crude oil evaluated here showed only a limited representation of such sulfoxide classes yet still formed stable emulsions. This suggests that other heteroatom classes, particularly oxygenated species and mixed N/O species, can compensate for the absence of sulfoxides. This highlights the complex and system-specific nature of interfacial stabilization. The lack of sulfoxide diversity may be attributed to the crude oil's different oxidation state and geological origin compared to that of the crude oils investigated in earlier studies, which directly examined isolated asphaltenes.[25,72]

The behavior of heteroatom classes under centrifugation emphasizes the distinct contributions of nitrogen- and oxygen-containing species to interfacial stability. $N_1[H]$ compounds increased in EPS and IMS over time but decreased in EPR and IMR at higher temperatures. This suggests that they have weak polarity and limited affinity for the interface compared to oxygenated acids.[28,60,73] Conversely, the abundance of the $N_2[H]$ class increased in EPR and IMR over time and at higher temperatures, consistent with greater structural complexity and hydrogen-bonding capacity enhancing their interfacial activity.

For the oxygenated classes, the $O_1[H]$ (phenolic-like species) class showed limited variation, indicating secondary interfacial activity. Their ability to form hydrogen bonds and $\pi-\pi$ stacking interactions may contribute to film rigidity; however, this association appears to be weakened at elevated temperatures due to reduced steric hindrance from wax-like components.[17] The $O_2[H]$ class (naphthenic and carboxylic acids) exhibited an opposite trend, becoming clearly enriched as time and temperature increased. In this class, low M_w acids

https://doi.org/10.1021/acs.energyfuels.5c03699
Energy Fuels 2025, 39, 18773−18790

dominate initial adsorption, while larger, more complex acids integrate into the interfacial film and confer viscoelastic and gel-like properties.[17,60,73,74] O_3 species displayed intermediate behavior, increasing with time but decreasing at higher temperatures, consistent with fragile adsorption.

Mixed $N_xO_y[H]$ classes also accumulated in IMR over time and at higher temperatures, albeit with slower kinetics than $O_2[H]$, which supports the preferential migration of small acids. Notably, sulfoxide-containing classes (e.g., O_4S), which are often reported to be critical for stability,[60,72,75] were absent in this oil; yet emulsions remained highly stable for months. This suggests that interfacial stabilization depends on the system, with oxygenated species being consistently important but expressed through different functional groups (e.g., fatty acids, naphthenic acids, diacids, asphaltene- or resin-bound acids).[17,74,76−78]

4. CONCLUSIONS AND PERSPECTIVES

This study used ESI(−) FT-ICR MS to provide molecular-level evidence of the influence of centrifugation parameters on the composition of the interfacial material in crude oil emulsions. Rather than being a static extract, it was demonstrated that IM is a dynamic fraction whose composition evolves over time and at different temperatures. This process involves the selective enrichment of naphthenic acids, phenolic compounds, and mixed nitrogen−oxygen species at the oil−water interface. Low-DBE carboxylic acids migrated rapidly, thereby lowering the interfacial tension; meanwhile, higher-DBE and more aromatic species accumulated more gradually to reinforce the interfacial film. These results highlight the distinct kinetic and thermodynamic contributions to interfacial stabilization, demonstrating that multiple chemical pathways can sustain emulsion stability even in the absence of sulfoxide classes that are traditionally considered essential.

By clarifying the roles of specific heteroatomic classes in interfacial enrichment, this work advances our mechanistic understanding of emulsion stability, providing a framework for evaluating how crude oil composition and processing conditions govern the formation of persistent emulsions. Such insights could inform the development of improved water−oil separation strategies and guide the design of more effective demulsification technologies, with direct implications for oil production and processing efficiency.

■ ASSOCIATED CONTENT

Supporting Information

The Supporting Information is available free of charge at https://pubs.acs.org/doi/10.1021/acs.energyfuels.5c03699.

Chromatogram of the studied crude oil emulsion sample using GC-FID, ESI(−) FT-ICR mass spectra, and processing data (DBE vs #C plots) and M_w (Da), class, DBE, and #C distribution for crude oil emulsion, crude oil, and their fractions obtained as a function of centrifugation time and temperature are reported (PDF)

■ AUTHOR INFORMATION

Corresponding Author

Wanderson Romão − *Federal University of Espírito Santo, Vitória 29075-910, Brazil; Federal Institute of Education, Science and Technology of Espírito Santo, Vila Velha 29106-010, Brazil;* orcid.org/0000-0002-2254-6683; Phone: +55027988575211; Email: wanderson.romao@ifes.edu.br

Authors

Luciara C. Souza − *Federal University of Espírito Santo, Vitória 29075-910, Brazil*

Lindamara M. Souza − *Federal University of Espírito Santo, Vitória 29075-910, Brazil*

Eliane V. Barros − *Federal Institute of Education, Science and Technology of Espírito Santo, Vitória 29040-780, Brazil*

Emily A. Carvalho − *Federal Institute of Education, Science and Technology of Espírito Santo, Vila Velha 29106-010, Brazil*

Marcos H. O. Petroni − *Federal University of Espírito Santo, Vitória 29075-910, Brazil*

Gabriely S. Folli − *Federal University of Espírito Santo, Vitória 29075-910, Brazil*

Cristina M. S. Sad − *Federal University of Espírito Santo, Vitória 29075-910, Brazil*

Danielle M. M. Franco − *Federal University of Goias, Goiania 74.690-631, Brazil*

Gabriel H. M. Dufrayer − *Federal University of Goias, Goiania 74.690-631, Brazil*

Boniek G. Vaz − *Federal University of Goias, Goiania 74.690-631, Brazil;* orcid.org/0000-0003-1197-4284

Marcio N. Souza − *Federal University of Rio de Janeiro, Rio de Janeiro 21941-853, Brazil;* orcid.org/0000-0003-0106-8034

Osvaldo Karnitz, Jr. − *Petróleo Brasileiro S.A, CENPES, Rio de Janeiro 21941-915, Brazil*

Luiz S. Chinelatto, Jr. − *Petróleo Brasileiro S.A, CENPES, Rio de Janeiro 21941-915, Brazil*

Marcia C. K. Oliveira − *Petróleo Brasileiro S.A, CENPES, Rio de Janeiro 21941-915, Brazil;* orcid.org/0000-0001-8820-8567

Valdemar Lacerda, Jr. − *Federal University of Espírito Santo, Vitória 29075-910, Brazil;* orcid.org/0000-0002-8257-5443

Complete contact information is available at: https://pubs.acs.org/10.1021/acs.energyfuels.5c03699

Funding

The Article Processing Charge for the publication of this research was funded by the Coordenacao de Aperfeicoamento de Pessoal de Nivel Superior (CAPES), Brazil (ROR identifier: 00x0ma614).

Notes

During the preparation of this work, the authors used ChatGPT from OpenAI in order to translate the document from Portuguese to English. After using the tool, the authors reviewed and edited the content as needed and took full responsibility for the content of the publication.

The authors declare no competing financial interest.

■ ACKNOWLEDGMENTS

The authors would like to thank CENPES/PETROBRAS (Rio de Janeiro, Brazil) for funding the research (process no. 2018/00110-4). The authors would also like to thank the Espírito Santo Research and Innovation Support Foundation (FAPES) for the financial support, the Petroleum Chemistry Competence Center and the Postgraduate Program in Chemistry at the Federal University of Espírito Santo (UFES, Espírito Santo,

Brazil), and the Federal Institute of Espírito Santo (IFES, Espírito Santo, Brazil).

REFERENCES

(1) Elsayed Abdel-Raouf, M. *Crude Oil Emulsions: Composition, Stability and Characterization*; Abdel-Raouf, M. E.-S., Ed.; InTechOpen: Rijeka, Croatia, 2012. DOI: 10.5772/2677.
(2) Umar, A. A.; Saaid, I. B. M.; Sulaimon, A. A.; Pilus, R. B. M. A Review of Petroleum Emulsions and Recent Progress on Water-in-Crude Oil Emulsions Stabilized by Natural Surfactants and Solids. *J. Pet. Sci. Eng.* **2018**, *165*, 673−690.
(3) Shafiei, M.; Kazemzadeh, Y.; Martyushev, D. A.; Dai, Z.; Riazi, M. Effect of Chemicals on the Phase and Viscosity Behavior of Water in Oil Emulsions. *Sci. Rep.* **2023**, *13* (1), No. 4100.
(4) Schramm, L. L. *Emulsions, Foams, and Suspensions: Fundamentals and Applications*; Wiley-VCH: Weinheim, Germany, 2006.
(5) Wang, Z.; Lin, X.; Rui, Z.; Xu, M.; Zhan, S. The Role of Shearing Energy and Interfacial Gibbs Free Energy in the Emulsification Mechanism of Waxy Crude Oil. *Energies* **2017**, *10* (5), No. 721.
(6) Kilpatrick, P. K. Water-in-Crude Oil Emulsion Stabilization: Review and Unanswered Questions. *Energy Fuels* **2012**, *26* (7), 4017−4026.
(7) Mohammadpour, M.; Malayeri, M. R.; Kazemzadeh, Y.; Riazi, M. On the Impact of Oil Compounds on Emulsion Behavior under Different Thermodynamic Conditions. *Sci. Rep.* **2023**, *13* (1), No. 15727.
(8) Alves, D. R.; Carneiro, J. S. A.; Oliveira, I. F.; Façanha, F.; Santos, A. F.; Dariva, C.; Franceschi, E.; Fortuny, M. Influence of the Salinity on the Interfacial Properties of a Brazilian Crude Oil−Brine System. *Fuel* **2014**, *118*, 21−26.
(9) Thomas, J. E. *Fundamentos de Engenharia de Petróleo*, 2nd ed.; Interciência: Rio de Janeiro, Brazil, 2004.
(10) Chen, G.; Tao, D. An Experimental Study of Stability of Oil−Water Emulsion. *Fuel Process. Technol.* **2005**, *86* (5), 499−508.
(11) Verruto, V. J.; Kilpatrick, P. K. Water-in-Model Oil Emulsions Studied by Small-Angle Neutron Scattering: Interfacial Film Thickness and Composition. *Langmuir* **2008**, *24* (22), 12807−12822.
(12) Adamson, A. W.; Gast, A. P. *Physical Chemistry of Surfaces*, 6th ed.; Wiley: New York, 1997.
(13) Spiecker, P. M.; Kilpatrick, P. K. Interfacial Rheology of Petroleum Asphaltenes at the Oil−Water Interface. *Langmuir* **2004**, *20* (10), 4022−4032.
(14) Orrego-Ruiz, J. A.; Medina-S, C. F.; Hinds, C. C.; Villar-García, Á.; Rojas-Ruiz, F. A. Determination by FT-ICR MS of the Role of Naphthenic Acids in the Stabilization of Alkali/Surfactant/Polymer Emulsified Effluents: A Field Study. *J. Pet. Sci. Eng.* **2019**, *179*, 192−198.
(15) Wu, X. Investigating the Stability Mechanism of Water-in-Diluted Bitumen Emulsions through Isolation and Characterization of the Stabilizing Materials at the Interface. *Energy Fuels* **2003**, *17* (1), 179−190.
(16) Jarvis, J. M.; Robbins, W. K.; Corilo, Y. E.; Rodgers, R. P. Novel Method To Isolate Interfacial Material. *Energy Fuels* **2015**, *29* (11), 7058−7064.
(17) Pereira, R. C. L.; Carvalho, R. M.; Couto, B. C.; de Oliveira, M. C. K.; Eberlin, M. N.; Vaz, B. G. Waxy Crude Oil Emulsion Gel: Chemical Characterization of Emulsified Phase Extract Components. *Energy Fuels* **2014**, *28* (12), 7352−7358.
(18) de Oliveira, M. C. K.; Miranda, L. R. O.; de Carvalho, A. B. M.; Miranda, D. F. S. Viscosity of Water-in-Oil Emulsions from Different API Gravity Brazilian Crude Oils. *Energy Fuels* **2018**, *32* (3), 2749−2759.
(19) Sad, C. M. S.; Santana, Í. L.; Morigaki, M. K.; Medeiros, E. F.; Castro, E. V. R.; Santos, M. F. P.; Filgueiras, P. R. New Methodology for Heavy Oil Desalination. *Fuel* **2015**, *150*, 705−710.
(20) Freitas, G. B.; Duncke, A. C.; Barbato, C. N.; de Oliveira, M. C. K.; Pinto, J. C.; Nele, M. Influence of Wax Chemical Structure on W/O Emulsion Rheology and Stability. *Colloids Surf., A* **2018**, *558*, 45−56.
(21) Petroni, M. H. O.; Corona, R. R. B.; Sad, C. M. S.; Ramos, R.; Castro, J. M.; Franco, L. G.; da Silva, M.; Elias, M. Z.; Castro, E. V. R. Role of Asphaltenes and Resins at the Interface of Petroleum Emulsions (W/O): A Literature Review. *Geoenergy Sci. Eng.* **2024**, *239*, No. 212932.
(22) Lalli, P. M.; Jarvis, J. M.; Marshall, A. G.; Rodgers, R. P. Functional Isomers in Petroleum Emulsion Interfacial Material Revealed by Ion Mobility Mass Spectrometry and Collision-Induced Dissociation. *Energy Fuels* **2017**, *31* (1), 311−318.
(23) Rojas-Ruiz, F. A.; Gómez-Escudero, A.; Pachón-Contreras, Z.; Villar-García, A.; Orrego-Ruiz, J. A. Detailed Characterization of Petroleum Sulfonates by Fourier Transform Ion Cyclotron Resonance Mass Spectrometry. *Energy Fuels* **2016**, *30* (4), 3050−3057.
(24) Rojas-Ruiz, F. A.; Rueda, M. F.; Pachón-Contreras, Z.; Villar-García, A.; Gómez-Escudero, A.; Orrego-Ruiz, J. A. Composition to Interfacial Activity Relationship Approach of Petroleum Sulfonates by Fourier Transform Ion Cyclotron Resonance Mass Spectrometry. *Energy Fuels* **2016**, *30* (6), 4663−4671.
(25) Wu, J.; Li, H.; Zhao, Q.; Zhou, B.; Lun, Z.; Zhang, Y.; Chung, K. H.; Shi, Q. Characterization of Crude Oil Interfacial Material by High-Resolution Mass Spectrometry. *J. Pet. Sci. Eng.* **2022**, *214*, No. 110509.
(26) Clingenpeel, A. C.; Rowland, S. M.; Corilo, Y. E.; Zito, P.; Rodgers, R. P. Fractionation of Interfacial Material Reveals a Continuum of Acidic Species That Contribute to Stable Emulsion Formation. *Energy Fuels* **2017**, *31* (6), 5933−5939.
(27) Ligiero, L. M.; Bouriat, P.; Dicharry, C.; Passade-Boupat, N.; Lalli, P. M.; Rodgers, R. P.; Barrère-Mangote, C.; Giusti, P.; Bouyssiere, B. Characterization of Crude Oil Interfacial Material Isolated by the Wet Silica Method. Part 1: Gel Permeation Chromatography Inductively Coupled Plasma High-Resolution Mass Spectrometry Analysis. *Energy Fuels* **2017**, *31* (2), 1065−1071.
(28) Norrman, K.; Olesen, K. B.; Zimmermann, M. S. L.; Fadhel, R.; Vijn, P.; Sølling, T. I. Isolation and Characterization of Surface-Active Components in Crude Oil—Toward Their Application as Demulsifiers. *Energy Fuels* **2020**, *34* (11), 13650−13663.
(29) Romão, W.; Barros, E. V.; Madeira, N. C. L.; Chinelatto, L. S.; de Oliveira, M. C. K.; Lacerda, V. Isolation of Interfacially Active Molecules from Brazilian Oils and Characterization by High-Resolution Analytical Techniques. *Braz. J. Chem. Eng.* **2024**, *41* (2), 669−680.
(30) Silva, J. d. C.; Pinto, F. E.; Souza, L. M.; Romão, W.; Loh, W.; Lucas, E. F. Chemical Characterization and Interfacial Activity of Molecules Isolated from Brazilian Oils by Adsorption onto Wet Silica Particles. *Energy Fuels* **2020**, *34* (11), 13552−13565.
(31) Silva, J. d. C.; Souza, L. M.; Fonseca, V. R.; Romão, W.; Loh, W.; Lucas, E. F. Isolation and Characterization of Interfacially Active Molecules from Asphaltene and Maltene Fractions. *Energy Fuels* **2023**, *37* (14), 10155−10165.
(32) Petroni, M. H. O.; Souza, L. M.; Barros, E. V.; Vieira, A. K. S.; Souza, L. C.; Monteiro, M. L.; Deus, J. S. R.; Cunha, P. H. P.; Sad, C. M. S.; Souza, M. N.; Karnitz, O. J.; Chinelatto, L. S.; de Oliveira, M. C. K.; Lacerda, V.; Romão, W. Optimization of Interfacial Material Isolation in Water−Oil Emulsions and Characterization by Fourier Transform Infrared Spectroscopy (FTIR): A Centrifugation Method Approach. *Energy Fuels* **2025**, DOI: 10.1021/acs.energyfuels.5c03137.
(33) ASTM International. *ASTM D4007−11, Standard Test Method for Water and Sediment in Crude Oil by the Centrifuge Method (Laboratory Procedure)*; ASTM International: West Conshohocken, PA, 2011.
(34) ASTM International. *ASTM D4377−06, Standard Test Method for Water in Crude Oils by Coulometric Karl Fischer Titration*; ASTM International: West Conshohocken, PA, 2006.
(35) ASTM International*ASTM D5002−05, Standard Test Method for Density and Relative Density of Crude Oils by Digital Density Analyzer*; ASTM International: West Conshohocken, PA, 2005.
(36) ASTM International. *ASTM D1250−13, Standard Guide for Use of the Petroleum Measurement Tables*; ASTM International: West Conshohocken, PA, 2013.

(37) ASTM International. *ASTM D7042−04, Standard Test Method for Dynamic Viscosity and Density of Liquids by Stabinger Viscometer*; ASTM International: West Conshohocken, PA, 2004.
(38) ASTM International. *ASTM D5853−17, Standard Test Method for Pour Point of Crude Oils*; ASTM International: West Conshohocken, PA, 2017.
(39) ASTM International. *ASTM D664−17, Standard Test Method for Acid Number of Petroleum Products by Potentiometric Titration*; ASTM International: West Conshohocken, PA, 2017.
(40) ASTM International. *ASTM D6470−04, Standard Test Method for Salt in Crude Oils (Potentiometric Method)*; ASTM International: West Conshohocken, PA, 2004.
(41) ASTM International. *ASTM D2549−17, Standard Test Method for Separation of Representative Aromatics and Nonaromatics Fractions of High-Boiling Oils by Elution Chromatography*; ASTM International: West Conshohocken, PA, 2017.
(42) Pereira, L. B.; Sad, C. M. S.; da Silva, M.; Corona, R. R. B.; dos Santos, F. D.; Gonçalves, G. R.; Castro, E. V. R.; Filgueiras, P. R.; Lacerda, V. Oil Recovery from Water-Based Drilling Fluid Waste. *Fuel* **2019**, *237*, 335−343.
(43) Coutinho, D. M.; França, D.; Vanini, G.; Mendes, L. A. N.; Gomes, A. O.; Pereira, V. B.; Ávila, B. M. F.; Azevedo, D. A. Rapid Hydrocarbon Group-Type Semi-Quantification in Crude Oils by Comprehensive Two-Dimensional Gas Chromatography. *Fuel* **2018**, *220*, 379−388.
(44) Rodrigues, É. V. A.; Silva, S. R. C.; Romão, W.; Castro, E. V. R.; Filgueiras, P. R. Determination of Crude Oil Physicochemical Properties by High-Temperature Gas Chromatography Associated with Multivariate Calibration. *Fuel* **2018**, *220*, 379−388.
(45) de Aguiar, D. V.; da Silva Lima, G.; da Silva, R. R.; Júnior, I. M.; Gomes, A. O.; Mendes, L. A. N.; Vaz, B. G. Comprehensive Composition and Comparison of Acidic Nitrogen- and Oxygen-Containing Compounds from Pre- and Post-Salt Brazilian Crude Oil Samples by ESI(−) FT-ICR MS. *Fuel* **2022**, *326*, No. 125129.
(46) Colati, K. A. P.; Dalmaschio, G. P.; de Castro, E. V. R.; Gomes, A. O.; Vaz, B. G.; Romão, W. Monitoring the Liquid/Liquid Extraction of Naphthenic Acids in Brazilian Crude Oil Using Electrospray Ionization FT-ICR Mass Spectrometry (ESI FT-ICR MS). *Fuel* **2013**, *108*, 647−655.
(47) Porto, C. F. C.; Pinto, F. E.; Souza, L. M.; Madeira, N. C. L.; Neto, Á. C.; de Menezes, S. M. C.; Chinelatto, L. S.; Freitas, C. S.; Vaz, B. G.; Lacerda, V.; Romão, W. Characterization of Organosulfur Compounds in Asphalt Cement Samples by ESI(+)FT-ICR MS and 13C NMR Spectroscopy. *Fuel* **2019**, *256*, No. 115923.
(48) Pinto, F. E.; Silva, C. F. P. M.; Tose, L. V.; Figueiredo, M. A. G.; Souza, W. C.; Vaz, B. G.; Romão, W. Evaluation of Adsorbent Materials for the Removal of Nitrogen Compounds in Vacuum Gas Oil by Positive and Negative Electrospray Ionization Fourier Transform Ion Cyclotron Resonance Mass Spectrometry. *Energy Fuels* **2017**, *31* (4), 3454−3464.
(49) Barros, E. V.; Dias, H. P.; Gomes, A. O.; Rodrigues, R. R. T.; Moura, R. R.; Sad, C. M. S.; Freitas, J. C. C.; Neto, A. C.; Aquije, G. M. F. V.; Romão, W. Study of Degradation of Acid Crude Oil by High-Resolution Analytical Techniques. *J. Pet. Sci. Eng.* **2017**, *154*, 194−203.
(50) Folli, G. S.; Souza, L. M.; Araújo, B. Q.; Romão, W.; Filgueiras, P. R. Estimating the Intermediate Precision in Petroleum Analysis by (±)Electrospray Ionization Fourier Transform Ion Cyclotron Resonance Mass Spectrometry. *Rapid Commun. Mass Spectrom.* **2020**, *34* (S3), No. e8861.
(51) Adermann, N.; Boggiano, J. *Composer, version 1.5.3*; Sierra Analytics: Pasadena, CA, USA, 2016.
(52) Lopes, V.; Vaz, B. G.; Rocha, Y. S.; Covas, T. R.; Queiroz Junior, L. H. K. *Thanus. Programa de Computador, BR512023002976−9*; INPI − Instituto Nacional da Propriedade Industrial: Brazil, 2023.
(53) Facanali, R.; Porto, N. A.; Crucello, J.; Carvalho, R. M.; Vaz, B. G.; Hantao, L. W. Naphthenic Acids: Formation, Role in Emulsion Stability, and Recent Advances in Mass Spectrometry-Based Analytical Methods. *J. Anal. Methods Chem.* **2021**, *2021*, No. 6078084.
(54) Liu, P.; Li, M.; Jiang, Q.; Cao, T.; Sun, Y. Effect of Secondary Oil Migration Distance on Composition of Acidic NSO Compounds in Crude Oils Determined by Negative-Ion Electrospray Fourier Transform Ion Cyclotron Resonance Mass Spectrometry. *Org. Geochem.* **2015**, *78*, 23−31.
(55) Shi, Q.; Zhang, Y.; Chung, K. H.; Zhao, S.; Xu, C. Molecular Characterization of Fossil and Alternative Fuels Using Electrospray Ionization Fourier Transform Ion Cyclotron Resonance Mass Spectrometry: Recent Advances and Perspectives. *Energy Fuels* **2021**, *35* (22), 18019−18055.
(56) Vaz, B. G.; Silva, R. C.; Klitzke, C. F.; Simas, R. C.; Lopes Nascimento, H. D.; Pereira, R. C. L.; Garcia, D. F.; Eberlin, M. N.; Azevedo, D. A. Assessing Biodegradation in the Llanos Orientales Crude Oils by Electrospray Ionization Ultrahigh Resolution and Accuracy Fourier Transform Mass Spectrometry and Chemometric Analysis. *Energy Fuels* **2013**, *27* (3), 1277−1284.
(57) Zhang, J.; Shan, H.; Chen, X.; Liu, W.; Yang, C. Synergistic Process for High Nitrogen Content Feedstocks Catalytic Cracking: A Case Study of Controlling the Reactions of Nitrogen Compounds in Situ. *Ind. Eng. Chem. Res.* **2014**, *53* (14), 5718−5727.
(58) Cui, D.; Chang, H.; Zhang, X.; Pan, S.; Wang, Q. Pyrolysis Temperature Effect on Compositions of Neutral Nitrogen and Acidic Species in Shale Oil Using Negative-Ion ESI FT-ICR MS. *ACS Omega* **2020**, *5* (37), 23940−23950.
(59) Mapolelo, M. M.; Rodgers, R. P.; Blakney, G. T.; Yen, A. T.; Asomaning, S.; Marshall, A. G. Characterization of Naphthenic Acids in Crude Oils and Naphthenates by Electrospray Ionization FT-ICR Mass Spectrometry. *Int. J. Mass Spectrom.* **2011**, *300* (2−3), 149−157.
(60) Stanford, L. A.; Rodgers, R. P.; Marshall, A. G.; Czarnecki, J.; Wu, X. A. Compositional Characterization of Bitumen/Water Emulsion Films by Negative- and Positive-Ion Electrospray Ionization and Field Desorption/Ionization Fourier Transform Ion Cyclotron Resonance Mass Spectrometry. *Energy Fuels* **2007**, *21* (2), 963−972.
(61) Pan, Y.; Liao, Y.; Shi, Q. Variations of Acidic Compounds in Crude Oil during Simulated Aerobic Biodegradation: Monitored by Semiquantitative Negative-Ion ESI FT-ICR MS. *Energy Fuels* **2017**, *31* (2), 1126−1135.
(62) Liao, Y.; Shi, Q.; Hsu, C. S.; Pan, Y.; Zhang, Y. Distribution of Acids and Nitrogen-Containing Compounds in Biodegraded Oils of the Liaohe Basin by Negative Ion ESI FT-ICR MS. *Org. Geochem.* **2012**, *47*, 51−65.
(63) Silva, A. L.; Pinto, F. E.; Souza, L. M.; Romão, W.; Loh, W.; Lucas, E. F. Identification and Quantification of Organic Compounds in Petroleum Fractions by GC-MS. *Energy Fuels* **2023**, *37* (5), 2643−2652.
(64) Orrego-Ruiz, J. A.; García, R.; Cundar Paredes, C. D.; Rojas-Ruiz, F. A. Characterization of Acid Species in Asphaltenic Fractions by Fourier Transform Ion Cyclotron Resonance Mass Spectrometry and Infrared Spectroscopy. *Energy Fuels* **2022**, *36* (24), 14852−14864.
(65) Niles, S. F.; Chacón-Patiño, M. L.; Chen, H.; McKenna, A. M.; Blakney, G. T.; Rodgers, R. P.; Marshall, A. G. Molecular-Level Characterization of Oil-Soluble Ketone/Aldehyde Photo-Oxidation Products by Fourier Transform Ion Cyclotron Resonance Mass Spectrometry Reveals Similarity Between Microcosm and Field Samples. *Environ. Sci. Technol.* **2019**, *53* (12), 6887−6894.
(66) Barrow, M. P.; McDonnell, L. A.; Feng, X.; Walker, J.; Derrick, P. J. Determination of the Nature of Naphthenic Acids Present in Crude Oils Using Nanospray Fourier Transform Ion Cyclotron Resonance Mass Spectrometry: The Continued Battle Against Corrosion. *Anal. Chem.* **2003**, *75* (4), 860−866.
(67) Son, S.; Kim, S.; Yim, Y.-H.; Kim, S. Reproducibility of Crude Oil Spectra Obtained with Ultrahigh Resolution Mass Spectrometry. *Anal. Chem.* **2020**, *92* (14), 9465−9471.
(68) Tadros, T. F. *Applied Surfactants*; Wiley-VCH: Weinheim, Germany, 2005. DOI: 10.1002/3527604812.

(69) Xu, B.; Kang, W.; Wang, X.; Meng, L. Influence of Water Content and Temperature on Stability of W/O Crude Oil Emulsion. *Pet. Sci. Technol.* **2013**, *31* (10), 1099−1108.
(70) Rogel, E. Asphaltene Aggregation: A Molecular Thermodynamic Approach. *Langmuir* **2002**, *18* (5), 1928−1937.
(71) Chang, X.; Liu, T.; Shi, B.; Liu, Z.; Zhang, P.; Xu, Y.; Chen, G. NSO-Bearing Compounds in Severely−Extremely Biodegraded Crude Oil Revealed by ESI(−) FT-ICR MS. *Energy Rep.* **2023**, *9*, 1077−1092.
(72) Qiao, P.; Harbottle, D.; Tchoukov, P.; Wang, X.; Xu, Z. Asphaltene Subfractions Responsible for Stabilizing Water-in-Crude Oil Emulsions. Part 3. Effect of Solvent Aromaticity. *Energy Fuels* **2017**, *31* (9), 9179−9187.
(73) Muller, H.; Pauchard, V. O.; Hajji, A. A. Role of Naphthenic Acids in Emulsion Tightness for a Low Total Acid Number (TAN)/High Asphaltenes Oil: Characterization of the Interfacial Chemistry. *Energy Fuels* **2009**, *23* (3), 1280−1288.
(74) Pauchard, V.; Sjöblom, J.; Kokal, S.; Bouriat, P.; Dicharry, C.; Muller, H.; Hutin, A. Role of Naphthenic Acids in Emulsion Tightness for a Low-Total-Acid-Number (TAN)/High-Asphaltenes Oil. *Energy Fuels* **2009**, *23* (3), 1269−1279.
(75) Ballard, D. A.; Chacón-Patiño, M. L.; Qiao, P.; Roberts, K. J.; Rae, R.; Dowding, P. J.; Rodgers, R. P.; Marshall, A. G. Molecular Characterization of Strongly and Weakly Interfacially Active Asphaltenes by High-Resolution Mass Spectrometry. *Energy Fuels* **2020**, *34* (11), 13966−13976.
(76) Andersen, S. I.; Mahavadi, S. C.; Abdallah, W.; Buiting, J. J. Infrared Spectroscopic Analysis of the Composition of an Oil/Water Interfacial Film. *Energy Fuels* **2017**, *31* (9), 8959−8966.
(77) Cañas-Jaimes, D.-L.; Cabanzo, R.; Mejía-Ospino, E. Comparison of Interfacial Tension Reduction in a Toluene/Water System by Colombian Crude Oil and Its Interfacially Active Components. *Energy Fuels* **2019**, *33* (5), 3753−3763.
(78) Rahham, Y.; Rane, K.; Goual, L. Characterization of the Interfacial Material in Asphaltenes Responsible for Oil/Water Emulsion Stability. *Energy Fuels* **2020**, *34* (11), 13871−13882.

https://doi.org/10.1021/acs.energyfuels.5c03699
Energy Fuels 2025, 39, 18773−18790